STUDY OF CHEMICALLY DEPOSITED THIN FILMS OF ZnO AND CdS

A Thesis

submitted to the

UNIVERSITY OF POONA

for the degree of

DOCTOR OF PHILOSOPHY

(IN CHEMISTRY)

By

S. D. SATHAYE

M. Sc.

National Chemical Laboratory,

Poona-8.

1972

C O N T E N T S

		Page
GENERAL INTRODUCTION		1
P A R T - I		
CHAPTER - 1 -	Introduction to ZnO	3
CHAPTER - 2 -	Experimental	24
CHAPTER - 3 -	Results	34
CHAPTER - 4 -	Discussion	57
REFERENCES		75
P A R T - II		
CHAPTER - 1 -	Introduction to CdS	79
CHAPTER - 2 -	Experimental	89
CHAPTER - 3 -	Results	97
CHAPTER - 4 -	Discussion	106
REFERENCES		114
SUMMARY		118

---000---

GENERAL INTRODUCTION

The electronic properties of noncrystalline solids have been attracting increasing attention during recent years. Valence semiconductors such as Ge and Si or chalcogenides such as As_2S_3, Sb_2S_3 have been prepared in amorphous or glassy states and their semiconducting properties studied in detail. However, transition metal oxides, which are known to show many interesting properties in the crystalline state, have not yet been studied in the amorphous state in much detail. In case of these oxides, a special attention has to be paid to the preparation method to get desired stoichiometric composition. This is rather important because any departure from stoichiometry brings about changes in conductivity which might mask the effect due to the noncrystalline nature. It is often difficult to maintain a control on the composition when high temperatures are used to prepare the material. Even the sputtering technique, which has been used to prepare amorphous thin films, seems to have failed to yield stoichiometric compounds.

We were, therefore, specially exploring the possibility of preparing thin homogeneous films of amorphous oxides from solution, at low temperatures. We have succeeded in preparing amorphous zinc oxide thin films and their properties are reported in this thesis. Also, the crystalline thin films of zinc oxide are prepared by this method using higher temperatures

and the properties of amorphous and crystalline films have been compared.

This new method of preparation of thin films when applied to prepare cadmium sulphide film was found to give films having the cubic structure. On the other hand, CdS films, prepared by conventional methods, have generally, the hexagonal structure and all attempts to prepare cubic CdS thin films have so far failed. Bube has reported the study on thin layers of cubic cadmium sulphide formed by decomposition of some organic compounds. However, for the formation of these layers, a binder was essential and hence the true properties of CdS could have been disturbed.

In this thesis, we present the study of crystalline and noncrystalline zinc oxide thin films and crystalline cadmium sulphide thin films. The thesis is divided in two parts. Part I deals with zinc oxide and Part II with cadmium sulphide. Each Part is divided in four Chapters. Chapter 1 in each case gives the work done so far in the respective areas, Chapter 2 on the experimental techniques, Chapter 3 on results and Chapter 4 on discussion followed by the bibliography.

A consolidated summary is given in the end.

PART - I

CHAPTER - 1 - INTRODUCTION TO ZnO

1.1.1. Zinc oxide has been studied in four different forms (1) single crystals, (2) thin films, (3) sintered pellets, and (4) sintered layers. The properties of zinc oxide are found to depend, to a considerable extent, on the form in which the substance is studied and also on the method of the preparation of the sample. Studies on single crystals are more reliable because of the absence of defects such as grain boundaries and voids. Sintered pellets and layers are studied mainly where the catalytic activity of zinc oxide is important. To know the effect of ambients, it is most useful to study zinc oxide in the form of thin films.

The electrical conductivity of zinc oxide has been studied in great detail. Other electronic properties studied are photoconductivity, Hall effect, luminescence, thermo-electric power, absorption in ultraviolet and infrared regions, etc. These properties have been studied under different ambient conditions of temperature, gas pressure, etc. They are helpful in elucidating the electronic conduction mechanism and the band structure of the material.

Amongst the factors which affect the electronic properties of zinc oxide, the following are more important: (1) form of the sample i.e. single crystal, thin film, etc., (2) method of preparation, (3) treatment before measurements, (4) temperature, (5) ambient conditions, such as the pressure of the gas in equilibrium with a sample, etc., (6) impurities.

1.1.2. PHYSICAL PROPERTIES

Zinc oxide has the hexagonal wurtzite structure[1] with lattice constants a = 3.2495Å, c = 5.206Å and c/a = 1.60. There are two molecules of ZnO in the unit cell and the atomic positions are:

Zn at [000], [1/3,2/3,1/2],

O at [00u], [1/3,2/3;u+1/2],

where u = 0.346.

Each atom is surrounded by a tetrahedron of four atoms of the opposite sort. The structure can be conveniently, though rather artificially, considered as composed of ZnO_4 or OZn_4 tetrahedra. The tetrahedra are stacked in a hexagonal closed packed array with the tetrahedra edges of alternate layers rotated through 180° about the 'c' axis.

Chemically deposited zinc oxide is a fine grained powder. The particle size is very small (of the order of one micron) and it has a large specific surface area. This property is useful in experiments where zinc oxide is used as a catalyst.

1.1.3. HISTORICAL BACKGROUND

Fritsch[2] measured the conductivity (σ) and Hall coefficient (R_H) of evaporated ZnO layers at low temperatures. The slopes of log σ vs 1/T and log V_H vs 1/T plots were found to be equal in magnitude.

Harrison[3] found a similar behaviour for crystals and for sintered samples. In addition, he studied the time dependence of conductivity. From his[4] work on Hall effect and conductivity, he concluded that the simple 'Wilson' semiconductor model was not able to explain the observations. The Hall curves were interpreted by a model considering (1) orbital degeneracy of the electrons attached to interstitial zinc atoms, (2) additional levels close to the impurity level and (3) traps, far below the donor level.

It is possible to justify this model if we assume that in zinc oxide, Zn^{+}, O^{-}, O^{--} species are present, the former two forming 'D' centres.

Heiland[5] in a series of papers reported the conductivity behaviour of thin zinc oxide layers and zinc oxide single crystals at different temperatures upto 300°C. He explained his results with the help of adsorption-desorption mechanism and came to the conclusion that the concentration of donors in a thin surface layer was lower than the concentration in the bulk.

Adsorption of gases on the surface of the material is of utmost importance when we consider the behaviour of zinc oxide, particularly in the temperature range of 20° to 600°C. In many cases reproducible results of conductivity were not observed because the gas in equilibrium with the surface was not controlled.

Stöckmann[6] observed that the conductivity increased with temperature upto 250°C(maximum) and then decreased to a minimum at 400°C. Above 400°C, the conductivity again increased. If the zinc oxide sample was preheated at 150° in hydrogen and conductivity measured, the maximum appeared at 150°C. If the sample was heated at 400°C in hydrogen and measurements done, two maxima appeared; one at 150°C and the other at 250°C.

Conductivity and Hall effect in zinc oxide single crystals doped with foreign atoms were studied by Kupprecht[7] in the temperature range of 65°K to 700°K. The carrier concentration and mobility values were comparable with the theoretically calculated figures.

Tischer[8] did his measurements on thin films of zinc oxide. He studied the reversible and irreversible zones of conductivity in different temperature ranges from 20°C to 500°C.

Morrison and Miller[9] measured the adsorption of O_2 on ZnO powder. Bevan and Anderson[10] studied the conductivity of sintered zinc oxide at high temperatures between 500°C and 1000°C. The results of Morrison et al.and Bevan et al. were in general agreement with each other.

Intemann and Stöckmann[11], Jander and Stamm[12] and Hahn[13] studied the conductivity of zinc oxide from 20°C to 700°C. The purpose of the study was to know the reversibility under different treatments of temperatures so as to explain the effect of

adsorption on samples and the part it played in the conduction mechanism.

H. Preier[14] studied the effect of annealing on the conductivity of thin zinc oxide films.

Glemza and Kokes[15] studied sintered zinc oxide pellets for adsorption of oxygen and conductivity changes with pretreatment of the sample and with changes in other parameters.

Stöckmann[6] measured the conductivity of zinc oxide evaporated films at temperatures ranging from 20°C to 800°C. At high temperatures, conductivity was independent of the sample history; on the other hand, at low temperatures, it was very much dependent on the pretreatment.

Heiland[5] studied the conductivity of zinc oxide single crystals which were preheated in different atmospheres and at different temperatures. Generally, heating in oxygen gave lower conductivity for zinc oxide while pretreatment at high temperatures in hydrogen increased the conductivity.

Hahn[13] showed that the conductivity was dependent on the relative thickness of grain boundary material formed during sintering. The Hall voltage on the other hand, was found to be dependent on the carrier concentration in the semiconducting zinc oxide grain.

Mollow[16] interpreted the effect of different heat treatments on single crystals of zinc oxide on their conductivity in the following way:

On the surface of the crystal there exists a layer whose conductivity is more than the bulk and its temperature dependence is smaller. At low temperatures, conductivity of this layer is measured. At higher temperatures, space charge is formed by the adsorbed oxygen on the surface, and the conductivity is reduced. At 300°C, oxygen is desorbed and conductivity increases. At 800°C, this conducting layer itself is removed and conductivity decreases to the bulk value. Adsorbed oxygen may create a field which attracts Zn^{+} to the surface to increase its conductivity.

Jander and Stamm[12] and Miller[17] studied compacts of ZnO powder and found the resistance to be high while Fritsch[2] found that on sintering the pellets, the resistance was reduced.

The effect of ambient atmosphere on the conductivity, thermoelectromotive force, Hall coefficient etc. of zinc oxide has been studied by several workers, as it is an important factor in controlling the properties. Obviously the aim of such studies has been to know the part played by adsorbed gas in the mechanism of conduction.

The dependence of conductivity and thermoelectric power of ZnO and Cu_2O on oxygen pressure was studied by Hogarth[18] at different temperatures.

Bevan and Anderson[11] carried out conductivity measurements in air and found that the method of sample preparation controlled the conductivity values to a large extent. Low oxygen pressure, on the other hand, gave similar values in spite of different sample origins.

Heiland[5] measured the conductivity of ZnO monocrystals from -183°C to 300°C. The conductivity decreased in presence of adsorbed oxygen. For such oxygenated crystals, he showed that the donors in the thin surface layer were less in number than in the interior.

Harrison[4] studied polycrystalline ZnO in greater details and showed that the part played by oxygen in conduction mechanism could not be explained as adsorption-desorption process. A new model called 'D' model which explained many observations was suggested.

Lander and Thomas[19] reported the conductivity of ZnO single crystals prepared by direct oxidation of zinc vapours at about 1200°C. The dependence of conductivity on hydrogen pressure was established and the relation suggested was $\sigma \propto P_{H_2}^{1/4}$, disagreeing from Mollow's results. They concluded

that the only way to explain the results was through the formation of OH^- ions at the surface by hydrogen-oxygen combination.

Ruppel, Gerristen and Rose[20] worked on finely divided ZnO powder layers and showed that the resistivity was close to that of the intrinsic ZnO. The explanation given was that the finely divided state appeared to allow surface adsorbed O_2 to stimulate the effect it would have, if it could be diffused into the volume of the bulk material.

Morrison[21] studied the change of conductivity of ZnO as a function of temperature in oxygen. According to his results, below 20°C, oxygen pressure had no effect on conductivity, while above 500°C, equilibrium between the processes at the surface and the bulk was established and the variation of conductivity was according to equation $\sigma = AP_{O_2}^{-1/4}$. At intermediate temperatures the results were complicated and probably dependent on the history of the sample.

Krusmayer[22] carried out the conductivity measurements on ZnO crystal surface in oxygen and also in vacuum. Conductivity changes were studied at 300°K. He concluded that the theoretically expected results from space charge layer formation theory and practical results agree.

Lander[23] studied Li doped crystals in a reducing atmosphere, and found that impurities acted as donors forming

LiO^{--} donor centres. In oxidising atmosphere Li acted as an acceptor, replacing Zn^{++} in the lattice.

Schulter et al.[24] used successive or simultaneous chemisorption of water vapour and oxygen while conductivity of ZnO was being measured. A mechanisms of reaction was suggested and compared to that given by Schwab.

Myasnikov[25] coated a quartz tube with thin layer of ZnO and observed that its electrical conductivity was smaller in oxygen than in vacuum. The difference was less if the frequency of electric current was more. The conductivity was found to decrease as the oxygen pressure increased, from 0.001 to 1 mm of Hg. The results were explained by chemisorption of O_2 on zinc oxide by electrostatic forces.

Cimino et al.[26] showed the positive influence of chemisorbed oxygen on the electrical conductivity of pure or doped ZnO powder. The formation of 'p' type inversion layer on the surface was suggested to explain the observations. Treatment in high vacuum at 450°C removed the p-type surface layer and n-type behaviour was observed.

Glemza and Kokes[16] suggested that the oxygen adsorption at high temperature was a two step process involving an unstable surface species as an intermediate. The authors worked on sintered pellets of ZnO measuring the conductivity as a function of temperature, adsorbed O_2, pretreatment and doping.

Watanabe and Wada[27] observed that the conductivity of ZnO powder was reduced by adsorbed O_2. The activation energy for conductivity (1.0 to 1.1 eV) was shown to be matching with the binding energy of the chemically adsorbed oxygen.

Hoffman[28] studied the reflectance and surface conductivity of ZnO crystals. He reported that the reflectance was altered by adsorbed oxygen.

J. Mak Nobbs[29] reported the effect of various atmospheric constituents on zinc oxide conductivity. Water vapour, ozone and atmospheric ions affected the conductivity to a large extent.

The conductivity of zinc oxide generally increases when irradiated by light or electrons. This is observed in layers, sintered samples and single crystals. If one examines the time dependence of rise in conductivity, it is easy to make out two distinguishable processes.

(1) A fast process - It is the one which raises the conductivity of sample rapidly to saturation value when the light is switched on. When the irradiation is stopped rapid fall to initial value of conductivity is observed.

(2) A slow process - Here, as against the fast process, the rise in conductivity is very sluggish. This state is maintained in vacuum until oxygen is introduced. Then the conductivity drops a little faster. These are shown in Fig. Nos. 1.1a and 1.1b.

SCHEMATIC VARIATION OF PHOTOCURRENT WITH TIME IN CASE OF FAST PROCESS (Thin layer) (1·1 a)[30]

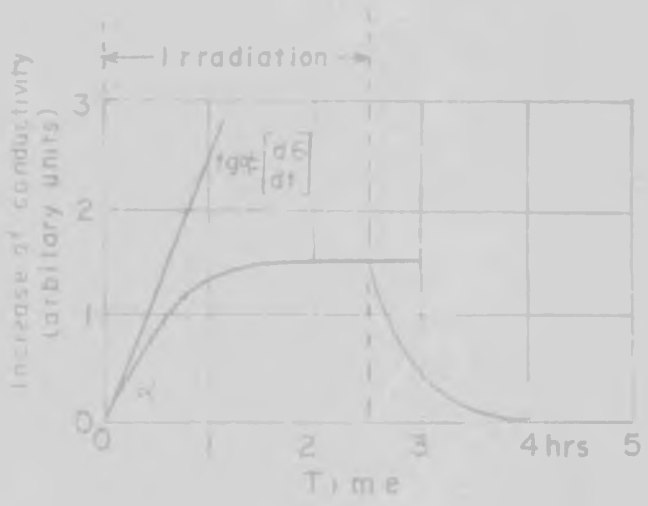

VARIATION OF CONDUCTIVITY WITH TIME, DURING LIGHT IRRADIATION IN SLOW PROCESS (Thin film) (1 1b)[30]

Fig 1·1a & 1 1b

The slow and fast processes in the photoconducting zinc oxide in the UV region was studied by Heiland[6], Weiss[31], Melnik[32], Collins and Thomas[33], and many others. The results are explained on the basis of a photo desorption process though all the observations could not be explained on this basis.

ESR measurements by Kasai[34] have shown the presence of a level, 0.8 ev deep, due to oxygen vacancy having a trapped electron.

Gray and Amigues[35] reported various trap levels in pure zinc oxide by thermally stimulated electron current measurements. The levels reported are at 0.12 to 0.15 ev (donors), 0.6 ev, 0.8 ev, 0.9 ev and 1.1 ev.

The optical properties such as reflectance or absorption give an idea about the band structure of a semiconductor. Many workers have studied these properties of ZnO. To mention one of them, Mollow[36] studied the optical absorption of thin films of zinc oxide. Also he reported the observations on the UV absorption of ZnO single crystals. The decomposition of zinc hydroxide was studied by Duval and M De-Clerk[37] using the differential thermal analysis technique. Zinc hydroxide was prepared by reacting ammonia gas with a zinc salt solution. The losses in weight were observed at 100°C, 200°C and 900°C. The explanation given was that at 100°C the adsorbed water as well as that formed from the decomposition of hydroxide was lost. At 200°C, the decomposition continued but not directly to zinc

oxide. After 200°C, a flat portion was said to be due to the formation of a stable basic carbonate of zinc which completely decomposed at 900°C. After 1000°C a stable portion was due to zinc oxide.

Other properties of zinc oxide which have been studied are thermoluminescence, photoluminescence, Hall effect, field effect, piezoelectric effect, etc.

Harrison studied the Hall effect in sintered ZnO and found that above 150°C the mobility varied as $\mu \propto T^{-3/2}$ where T is the absolute temperature. Heiland[6], Krusmayer, studied the field effect in ZnO. Hoffmann and Mollow[38] studied the variation of luminescence yield as a function of absorption of oxygen.

Kröger and Mayer[39] studied the edge emission in ZnO.

1.1.4. MECHANISMS

To explain the observations of conductivity and photoconductivity in general and the effect of ambient gases in particular, many models have been suggested. It would not be out of place to discuss some of these at this stage.

Electron transfer theory of chemisorption

Morrison suggested the energy diagram, as shown in figure 1.2, to explain conductance, photoconductance, fluorescence and the absorption of hydrogen.

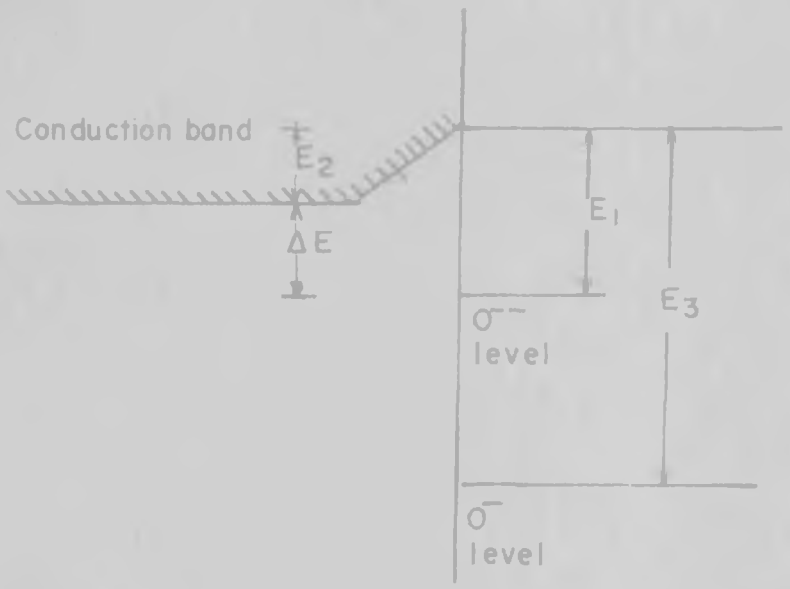

E_2 = Barrier created by adsorbed oxygen for electron to transfer from bulk to surface

E_1 = Chemically adsorbed O_2 level (O^{--})

E_3 = Physically adsorbed O level (O^{-})

Fig 12

ENERGY LEVEL DIAGRAM FOR ZnO as SUGGESTED BY S.R.MORRISON

The time dependence of conductivity in zinc oxide is explained by this model as follows:

As the temperature is increased, O^{--} levels lose electrons to conduction band and conductance rises. As the equilibrium with respect to O^{--} levels is attained, conductance vs time curve goes through maximum. Then the influence of O^{-} levels dominate the properties reducing the conductance.

Barry and Stone's Model[40]

This model is basically different from the one suggested by Morrison. The assumptions are:

(1) At low temperature effective oxygen levels are O^{-} or O_2^{-} rathert than O^{--}.

(2) At higher temperatures O^{--} levels predominate.

They showed how the time dependence of conductivity observed in Morrison's experiment could be easily explained as well as photoconductivity in zinc oxide. The model is based on adsorption-desorption experiments of oxygen on zinc oxide.

Schwab's Model[41]

The model proposed by Schwab is based on the part played by water vapour in photocatalytic activity of ZnO.

Oxygen is chemisorbed by ZnO at moderate temperatures as O_2^{-}, O^{-} or O^{--} because electrons from donors are available to

combine with the atmospheric oxygen. When ZnO is illuminated, the possible reactions are:

(1) $O_2 + e^- \rightarrow O_2^-$.

$O_2^- + H_2O \rightarrow HO_2 + OH^-$.

(2) $O_2 + e^- \rightarrow O_2^-$

$O_2^- + H_2O \rightarrow HO_2^- + OH$

$HO_2^- + H_2O \rightarrow H_2O_2 + OH^-$

(3) $1/2O_2 + e^- \rightarrow O_{ads}^-$.

$O^- + H_2O \rightarrow OH + OH^-$

(4) $OH^- + Zn^{++} \rightarrow Zn^+ + OH$.

(5) $OH + OH \rightarrow H_2O_2$.

(6) $2H_2O_2 \longrightarrow 2H_2O + O_2$.

Reaction (5) is possible only on illumination.

Arghiropoulos and Tischner Model[42]

Assumption - Due to the adsorbed oxygen at the surface, a strong electric field is created which is able to draw the interstitial zinc ions from the bulk to the surface which can make electrons available for conduction. Secondly, electrons are consumed by the atmospheric oxygen getting chemisorbed at the zinc oxide surface.

At low temperatures, reaction 1 dominates, to give a maximum in the log σ_v-1/T plot. At higher temperatures,

second reaction predominates, hence the resistance increases to give a minimum in the log σ vs 1/T curve.

Diffusion Model

Fritzsche[43] suggested that many of the observations on ZnO could be explained by considering absorption of oxygen by samples as against adsorption as considered by other workers. Instead of the concept of barrier formed by O_2, he used the idea of diffusion of oxygen in and out of the sample to explain the results.

The mechanisms mentioned above to describe the various properties of zinc oxide are based on the assumption that the zinc oxide is in the crystalline form. These mechanisms may not work if the noncrystalline zinc oxide properties are to be explained. Following is the review of the work done on amorphous semiconducting thin films. This may be useful in developing the mechanism to explain the properties of amorphous semiconductors.

The general method of preparation of amorphous thin films is vacuum evaporation on substrates held at sufficiently low temperatures. Elements deposited by such method are, B, C, Ge, Si, Se, Te, etc. and compounds are SiC, InSb, GaSb, GaAs, InSe, In_2Se_3, GeTe, SnTe, As_2S_3, As_2Te_3, etc. Many

alloys have also been studied. Some examples are Ge_xTe_{1-x}, $As_2Te_{3y}(Si,Ge)_x$. Though contamination is very low in this method of preparation of thin films, attention has to be paid to the following facts:

(1) Changes in chemical composition by selective evaporation.

(2) Dissociation of compounds or alloys.

(3) Incomplete recombination on the substrate in case of alloys and compounds.

Another method used for preparing semiconducting amorphous thin films is cathodic sputtering of a bulk sample. Films of the compounds ZnO and elements and alloys like Ge, GeTe, $As_2Te_{3y}(Ge,Si)_x$ are formed by this method. The advantages of this method are:

(1) Easy control on deposition parameters.

(2) Changes in chemical composition are less, but these films include notable amounts of gases.

Radio frequency discharges through gases is another interesting way of getting the thin semiconducting amorphous films. Radio frequency through silane, for instance, forms amorphous Si film or the proper mixture of ammonia and silane forms amorphous Si_3N_4 films.

Electrolysis and chemical precipitation have also been used to obtain the amorphous films of Sb, Ge, As, etc.

A comment on the film structure is necessary because the film may be completely amorphous or partially crystallised. When the film is formed, the conditions are such that no crystallisation or only partial crystallisation takes place. For example, the necessary energy for atoms to rearrange may not be available or the foreign atoms may stop the process of crystallisation. Atomic structure in the film is characterised by the absence of long range ordering. However, sometimes the chain structure and some structures having definite regular arrangement but with only short range ordering have been observed.

The energy band structure of semiconducting amorphous films is expected to be isotropic in view of the isotropy in their macroscopic properties. The band edges are smeared out as against the sharp band edges in crystalline band edges because of the structural fluctuations and 'tails' of localised states are formed in the forbidden gap. Such tails may overlap forming highest density of states somewhere near the middle of the gap where Firmi level is expected in case of crystalline intrinsic semiconductors.

The study of the optical properties in amorphous semiconducting thin films is interesting. It is usually observed

that a shift of edge compared with that in the corresponding crystal takes place. Also, in case of alloys, it has been observed that the edge matches well with the gap obtained from electrical conductivity measurements showing that the optical absorption is due to the excitation of valence electrons across the band gap.

In Ge films the edge is exponential when the film is amorphous. As the film is annealed it becomes comparable to crystalline Ge edge. Similar situation is observed in 'B' films. Amorphous Si, Se, Te, films have also been studied.

As evident from the above description, the band structure is more or less maintained in amorphous semiconductors, but may have slight modifications and this will have definite effect on the electrical transport also. It may be stated that still the electrical transport is by electrons although the transport formulae may not be the same as in the crystalline semiconductors. The concept of Fermi Level is used for the explanation of electrical transport and the position of Fermi Level is used to define the amorphous semiconductor to be 'n' or 'p' type. The three principal mechanisms are as follows:

(1) At high temperatures electrons from valence band will be excited to conduction band and a hole created in valence band. Both will contribute to electrical transport and Fermi Level will be at the middle of band gap.

(2) At low temperatures the Fermi Level may move to one of the band edges considering the extended states (tails). The position of Fermi Level will decide the type of conductivity. At very low temperatures, hopping of electrons between the localised states near the Fermi Level may predominate.

This, of course, is a rough way of explaining the electrical transport phenomenon because no concrete theories have been developed for amorphous semiconductors. The experimental data on piezoresistance, thermoelectric power, magnetoresistance and high field conductivity is being collected. All the effects observed, are explained so far in terms of the movement of Fermi Level in the forbidden gap. Measurements of Hall effect have been carried out in only a few cases.

In conclusion, it can be seen that the study of amorphous solids as thin films have contributed appreciably to our knowledge about these solids which sometimes could not be prepared otherwise. Also, the study, so far done in this field is limited to materials having low band gap values. It should be interesting, therefore, to know the behaviour of wide band gap semiconductors such as ZnO in the amorphous state. Furthermore, in this thesis we describe a new method of the preparation of thin films which has so far not been used to prepare and study thin amorphous films.

CHAPTER - 2 - EXPERIMENTAL

1.2.1. PREPARATION OF THIN FILMS OF ZINC OXIDE

Thin films of zinc oxide were prepared by the decomposition of zinc hydroxide thin films formed on silica or glass substrate. The method of preparation of zinc hydroxide thin films is as follows:

Zinc sulphate (AR) solution in distilled water (1%) was taken in a shallow dish (Fig. No. 1.3). (We found that a variation in the initial concentration beyond 1% did not affect the properties of the thin films of zinc oxide finally obtained by decomposition. At much lower concentrations, however, films were not formed). A glass plate was kept dipped in this solution with an arrangement to lift it out when desired. The assembly was enclosed in an ammonia atmosphere for a few minutes. A thin layer of zinc hydroxide was formed at the surface of the solution. Care was taken that no precipitation inside the solution took place. The glass substrate which was kept in the solution was lifted up. In this process, the film was collected on the surface of the glass slide. The slide was then dipped in distilled water where the film started refloating and the soluble impurities were washed away. The film was picked up again and the process of washing was repeated two or three times. Finally, the film was collected on a silica or a glass substrate, dried and stored in a dessicator.

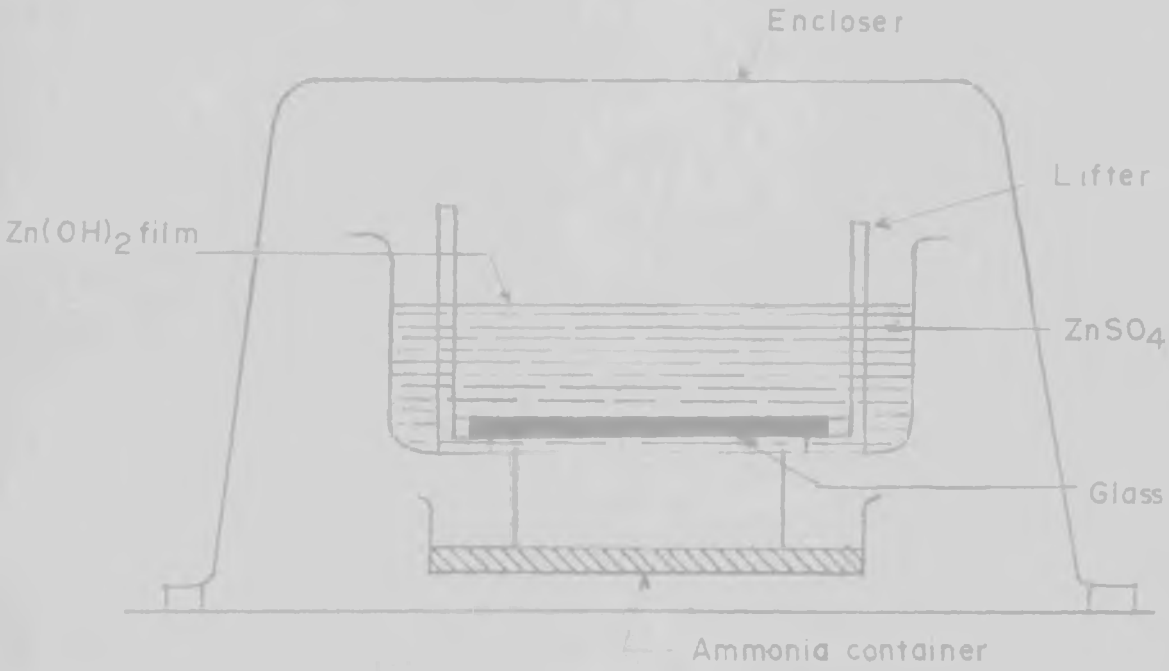

Fig I. 3 ARRANGEMENT FOR THE PREPARATION OF $Zn(OH)_2$ THIN FILM

1.2.2. X-RAY DIFFRACTION STUDY

The material of the film prepared by the method given above was collected by scraping and was heated in air at 140°C, 340°C, 450°C, 850°C and 1000°C.

The material was powdered in an agate mortar and was examined by the x-ray powder diffraction technique. Cu-K_α radiation was used (λ = 1.5405Å) for all experiments. The values of interplanar spacing, d, were calculated using the formula $\lambda = 2d \sin\theta$ where λ = wave length of x rays used, d = interplanar distance, θ = Bragg angle.

1.2.3. DIFFERENTIAL THERMOGRAVIMETRY

Differential thermal analysis and differential thermogravimetry techniques have become important tools to investigate the effect of temperature on different compounds. TG records the weight changes taking place in compounds while heating and gives an idea about the intermediate products formed during the decomposition reaction. The thermal data obtained from these curves are equally important for the interpretation of the nature of reactions. The DTA-TG curves are known to be affected by the following factors: (1) furnace heating rate, (2) recording chart speed, (3) furnace atmosphere, (4) geometry of the sample holder and furnace, (5) sensitivity of the recording mechanism, (6) amount of sample, (7) particle size, (8) solubility

of evolved gases in sample, (9) heat of reaction, (10) thermal conductivity. To obtain the maximum sensitivity and reproducibility a proper control on these factors had to be maintained. 200 mgms. of zinc hydroxide powder was used in each run. The sample was kept in an alumina crucible. The TG, DTG and DTA analyses were done using a MOM Budapest derivatograph.

1.2.4. CONDUCTIVITY MEASUREMENTS

Films of zinc hydroxide were prepared as described earlier and heated at 140°C, 340°C, 450°C, 850°C and 1000°C. Aqua dag electrodes were applied on the top surface of these films with the spacing of about 5 mm. between the inner edges of the aqua dag coating. The sample enclosure consists of a silica tube closed at one end having a B24 male joint at the other end. B-24 female joint is made up of corning glass and has a side tube with B-14 male joint attached to it. Through this B-14 joint, the system can be connected to a vacuum unit. In the walls of B-24 female joint, two copper wires and one each of chromel and alumel wires are sealed. The seals are leak proof at a vacuum of the order of 10^{-4} torr. Fig 1.4

The chromel-alumel junction is fixed inside the tube so that it can be placed near the sample. Two copper wires are joined to the two platinum wires which are fixed to the two stainless steel blocks.

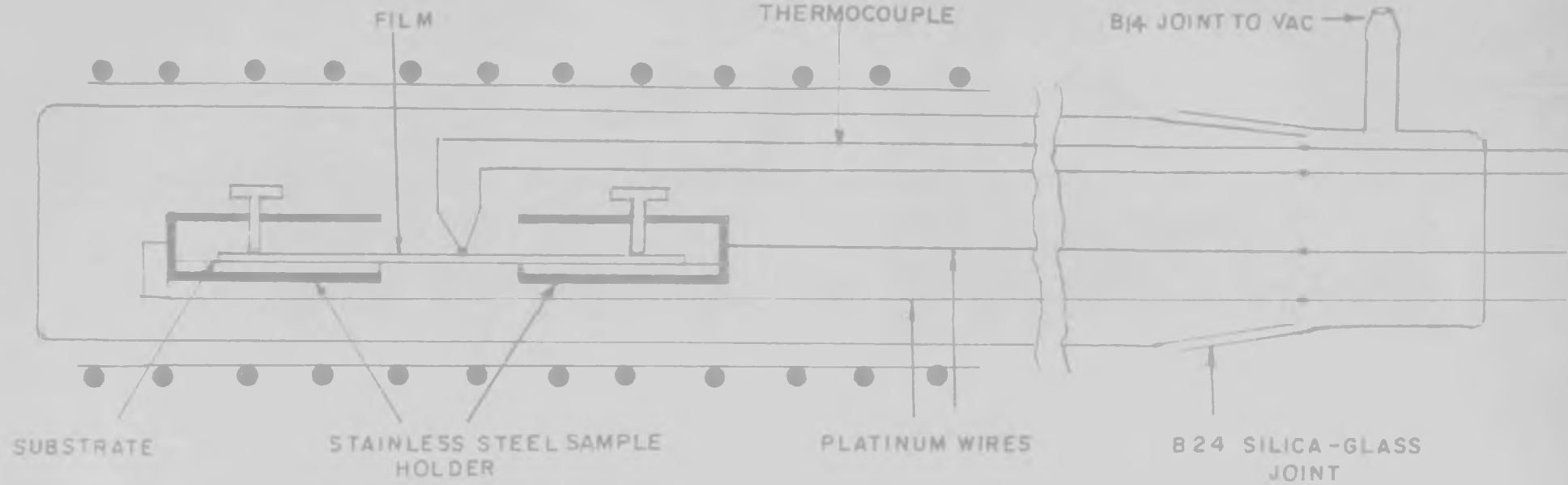

Fig 1-4 ARRANGEMENT FOR CONDUCTIVITY MEASUREMENTS

The film holder consists of two stainless steel blocks having an arrangement to fix the film electrodes with the help of screws. The two blocks do not have direct electrical contact.

After fixing the film in two blocks and placing the thermocouple junction on the film, the assembly was inserted in the silica tube described earlier. With this arrangement we could measure the resistance of the film between two copper wires and the thermocouple voltage which, in turn, gave the temperature of the sample. Fig 1.5

A furnace was constructed by winding Kanthal 'A' wire of 18 gauge on a 30 mm. diameter silica tube provided with a proper thermal insulation. To adjust and control the temperature of the furnace to any desired value upto 900°C, the input voltage was given through a temperature controller [Fallbugel-Regler Medin H; supplied by Hartmann and Braunn, Frankfurt, W. Germany].

The sample holder silica tube was inserted in the furnace so that the film was in the adjusted and controlled constant temperature zone. The electrical resistance measurements were carried out on a RIE meter [Leeds and Northrup, Model No. Cat. 5620].

Conductivity measurements could be done in vacuum with the same arrangement. A B-14 joint was used to join the assembly to vacuum line.

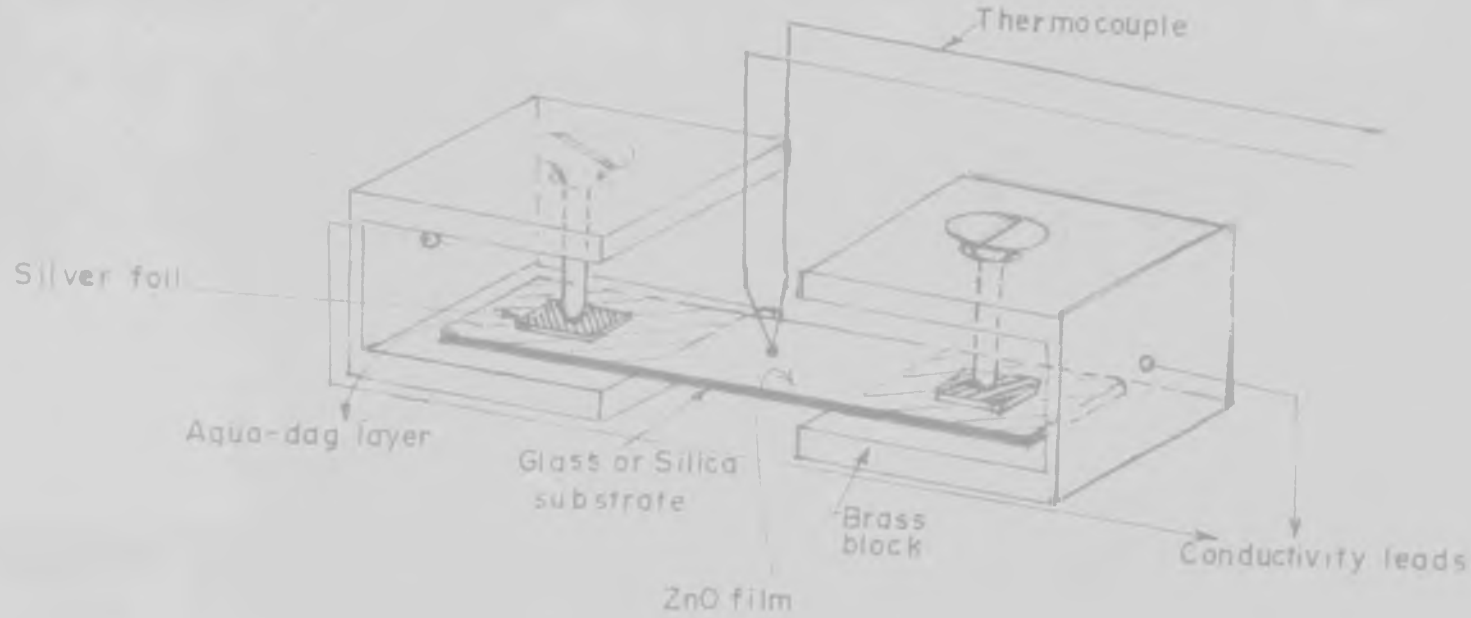

Fig 1·5 SAMPLE HOLDER FOR ZnO THIN FILM CONDUCTIVITY MEASUREMENTS

1.2.5. MEASUREMENTS IN HYDROGEN

The tube having the sample was evacuated and then hydrogen was allowed inside the tube. Again the tube evacuated and hydrogen allowed inside. The stopcock which allowed hydrogen inside, was closed and the tube heated to 500°C.(Fig. No. 1.6). Sample was then cooled inside the tube itself and again slowly heated to 500°C when the resistance was measured at different temperatures.

1.2.6. MEASUREMENTS IN OXYGEN

The sample tube was flushed with oxygen as described above and then the stop cock was closed. The temperature was adjusted at 200°C, 300°C or 400°C and kept constant; while by partial evacuation the oxygen pressure inside the tube was adjusted to the desired values. The resistance was measured at each oxygen pressure. Care was taken for the equilibrium pressure to attain i.e., it was seen that constant reading for resistance was obtained.

1.2.7. ULTRAVIOLET ABSORPTION

The UV absorption by the films heated at different temperatures was studied as follows: The film of zinc hydroxide was taken on an optically flat silica slide. A similar slide was used as a 'blank' and the absorption curve was obtained by scanning from 400 to 700 mm., on a Beckmann 350 spectrophotometer.

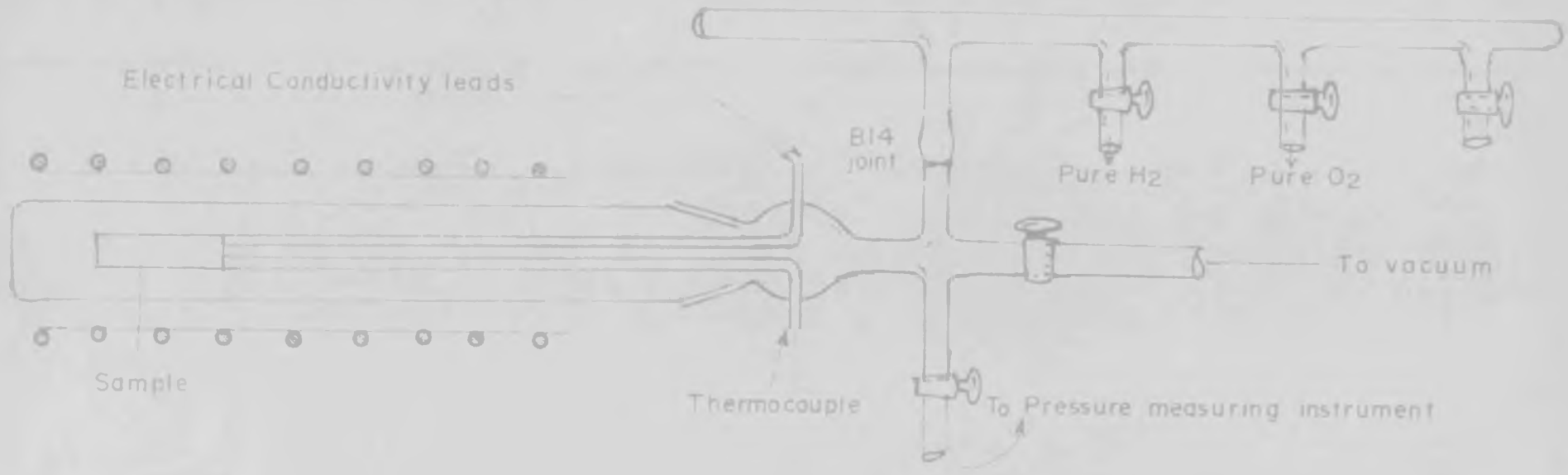

Fig 1.6 MEASUREMENTS OF CONDUCTIVITY IN PRESENCE OF DIFFERENT AMBIENT GASES

After this testing the film was heated at 300°C with blank and again the UV absorption was studied as above. Similar measurements were carried out after heating the film at different temperatures upto 850°C.

These curves were used to find out the possible band gap of the material tested.

CHAPTER - 3 - RESULTS

1.3.1. DIFFERENTIAL THERMAL ANALYSIS AND DIFFERENTIAL THERMOGRAVIMETRY

The curves obtained for DTA and DTG have been shown in Fig. No. 1.7. The weight of the powder was 200 mgms. when the experiment was started. The following are the important features of the results:

(1) Around 125°C, a major loss in weight (17%) was observed. The loss was however gradual starting at 70°C and ending at 210°C.

Simultaneously, the heat change is shown in DTA curve. As the peak is below the reference line, endothermic reaction is indicated.

(2) The substance loses weight further in three steps; at 280°C, 400°C and 470°C. The losses being 9%, 2% and 2% respectively. Associated heat changes with these weight losses are shown in DTA curve.

At 280°C, a sharp endothermic peak is observed. At 400°C, the peak is not as sharp as that at 280°C; and the one at 570°C shows very slow change in the enthalpy of the substance.

(3) A stable portion from 520°C to 860°C is observed where no heat or weight change occurs.

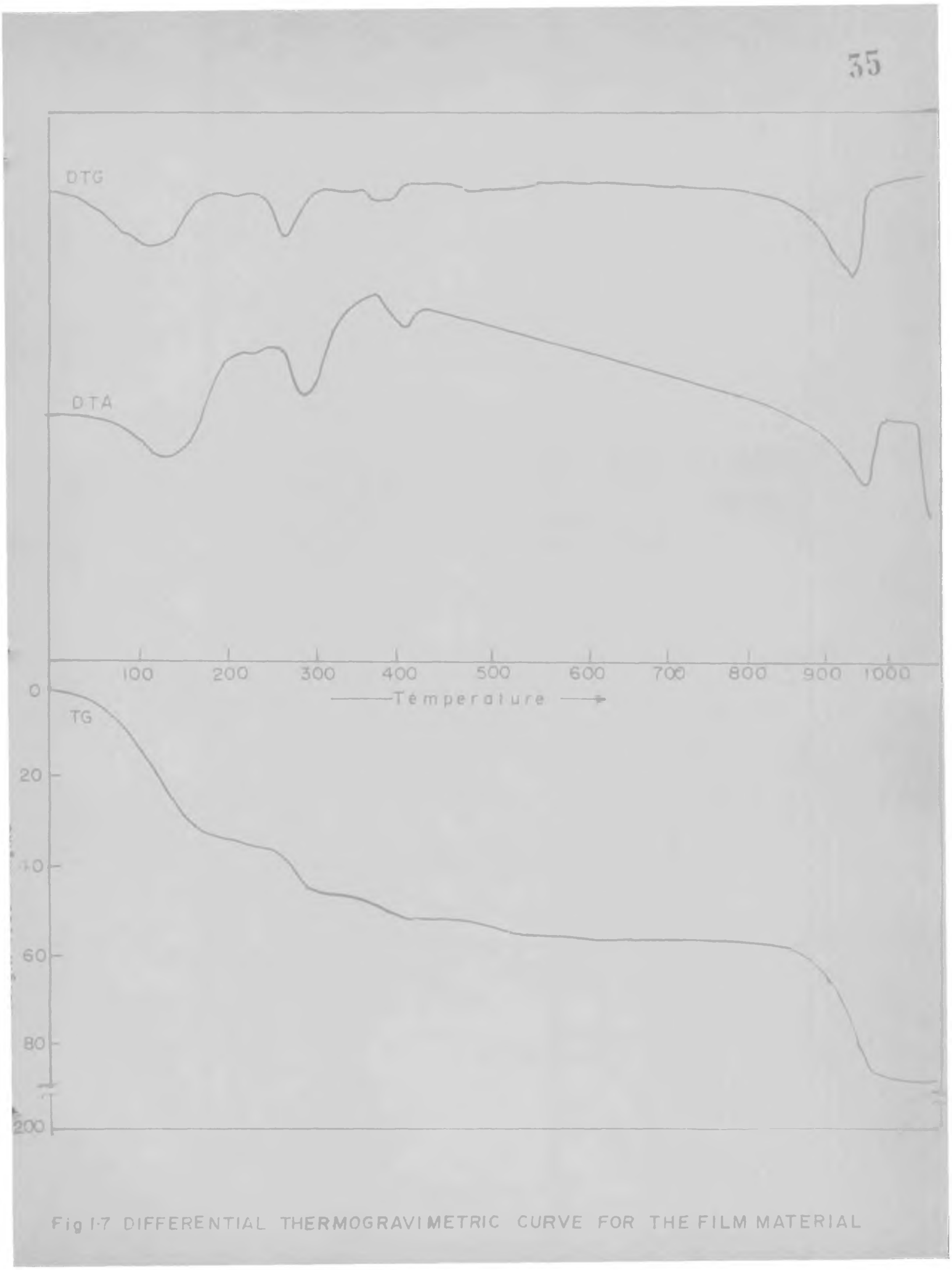

Fig 1·7 DIFFERENTIAL THERMOGRAVIMETRIC CURVE FOR THE FILM MATERIAL

(4) Finally, a sharp major loss in weight is shown, with peak at 970°C. The substance starts losing weight at 890°C and the loss stops at 1000°C. Corresponding to this, very sharp peak at 950°C is shown in the DTA graph. The reaction is an endothermic one. After 1000°C, a straight line is observed indicating that a stable phase has been formed.

The observations given above suggest that the original composition is not $Zn(OH)_2$ because, if it were so, after the loss of water at 125°C, weight would not have changed. The original composition, therefore, as suggested by Duval et al[37] may be $Zn(OH)_2.CO_2.xH_2O$.

Reaction may be as follows:

$$Zn(OH)_2.CO_2.xH_2O \rightarrow ZnO.CO_2 + YH_2O$$

Further losses at 280°C, 400°C and 470°C are not major. These may be explained due to further loss in water and perhaps part of adsorbed CO_2.

The basic carbonate formed decomposes at 1000°C giving out CO_2 as a reaction product and a stable phase of ZnO is formed shown by a straight line after 1000°C.

1.3.2. X-RAY STUDY

The main observations of the x-ray studies are as follows:

(1) No diffraction lines could be observed from the films heated at 220°C or 320°C.

(2) Very faint lines could be seen in x-ray diffraction patterns from samples heated at 450°C. Approximate 'd' values are given below.

(3) Clean diffraction lines could be seen in x-ray patterns from samples heated at 850°C.

No.	Calcd. 'd' values film heated at 850°C	'd' values for ZnO in ASTM cards	Film heated at 450°C
1.	2.80	2.816	2.81
2.	2.59	2.602	2.59
3.	2.46	2.476	2.46
4.	1.90	1.911	
5.	1.62	1.626	1.62
6.	1.47	1.477	
7.	1.38	1.379	
8.	1.36	1.359	
9.	1.24	1.225	
10.	1.93	1.0929	
11.	1.066	1.0639	
12.	1.042	1.0422	
13.	1.014	1.0168	
14.	0.976	0.9764	

The observed 'd' values from the sample heated at 850°C agree with those reported for ZnO. No additional lines are observed. The diffraction pattern is shown in Fig. No. 1.8.

Fig. 1.8. X ray diffraction pattern of ZnO.

It is observed that the ZnO film does not crystallise unless heated upto 450°C or above. The powder of the film heated at 450°C shows very faint lines in the pattern and the corresponding 'd' value do match with the 'd' values of ZnO 'wortzite' pattern suggesting the presence of only ZnO phase. No other crystalline phase is found to be formed.

1.3.3. ULTRAVIOLET ABSORPTION STUDY

Films heated upto 300°C did not show the absorption edge in the range 340-900 nm. Absorption edge at 375 nm. was shown by the film heated at 360°C. The absorption edge shifted towards longer wave length as the film was heated at higher temperature. The film heated at 850°C shows the absorption edge at 380 nm. The actual curves are shown in Fig. No. 1.9.

Films heated at higher temperatures do not show any further change in the position of the absorption edge.

Another interesting observation is that the percentage absorption increases as the crystalline nature of the film increases.

1.3.4. CONDUCTIVITY (IN AIR)

Figure 1.10 shows the plots of log R vs 1/T for the film heated at 140°C for 1 hour and for 15 hours (A and B respectively). Fig. 1.11 shows similar graphs for the films

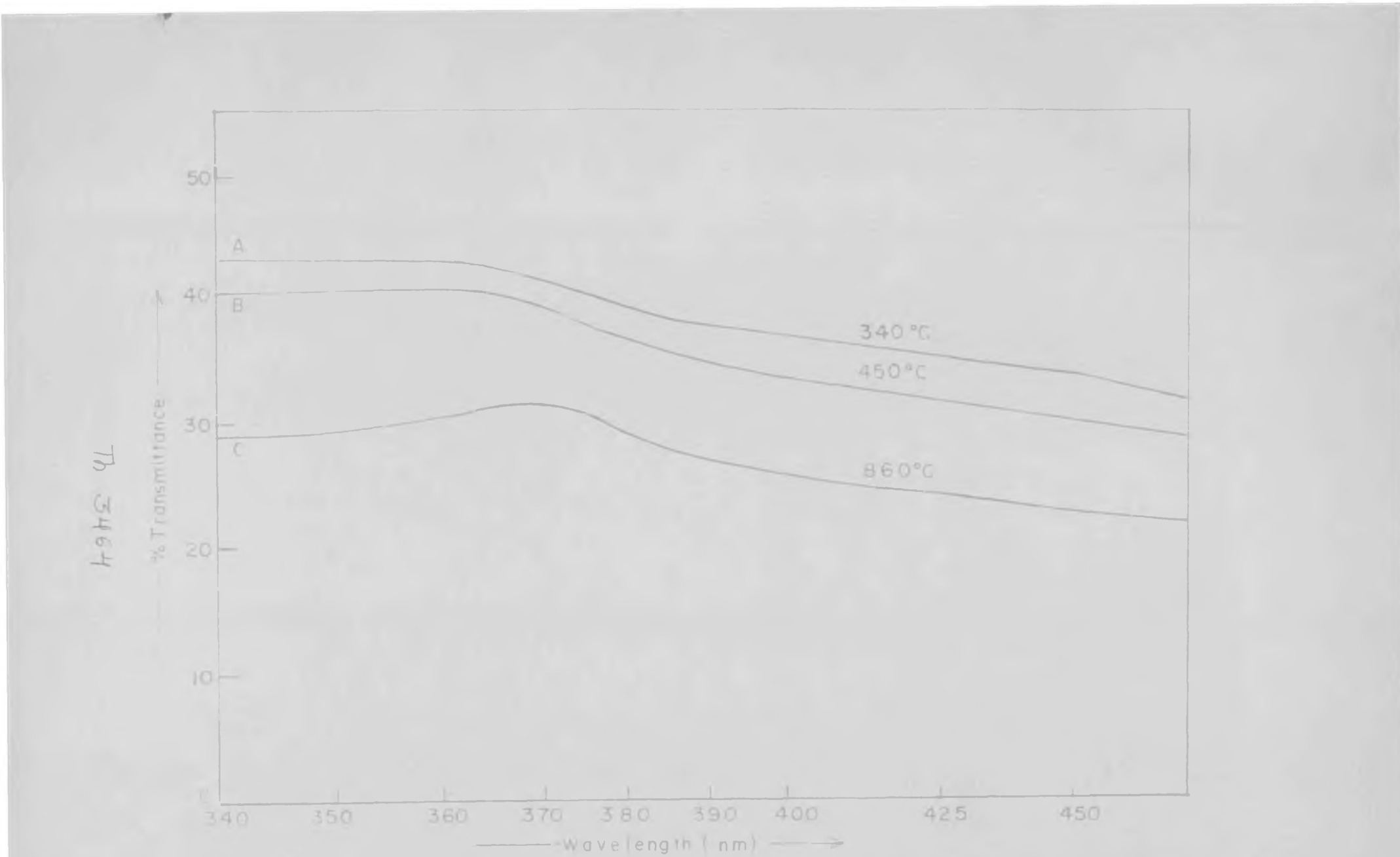

Fig 1-9 ABSORPTION IN UV BY ZnO THIN FILMS PREPARED BY HEATING $Zn(OH)_2$ AT 340°C, 450 °C 860 °C

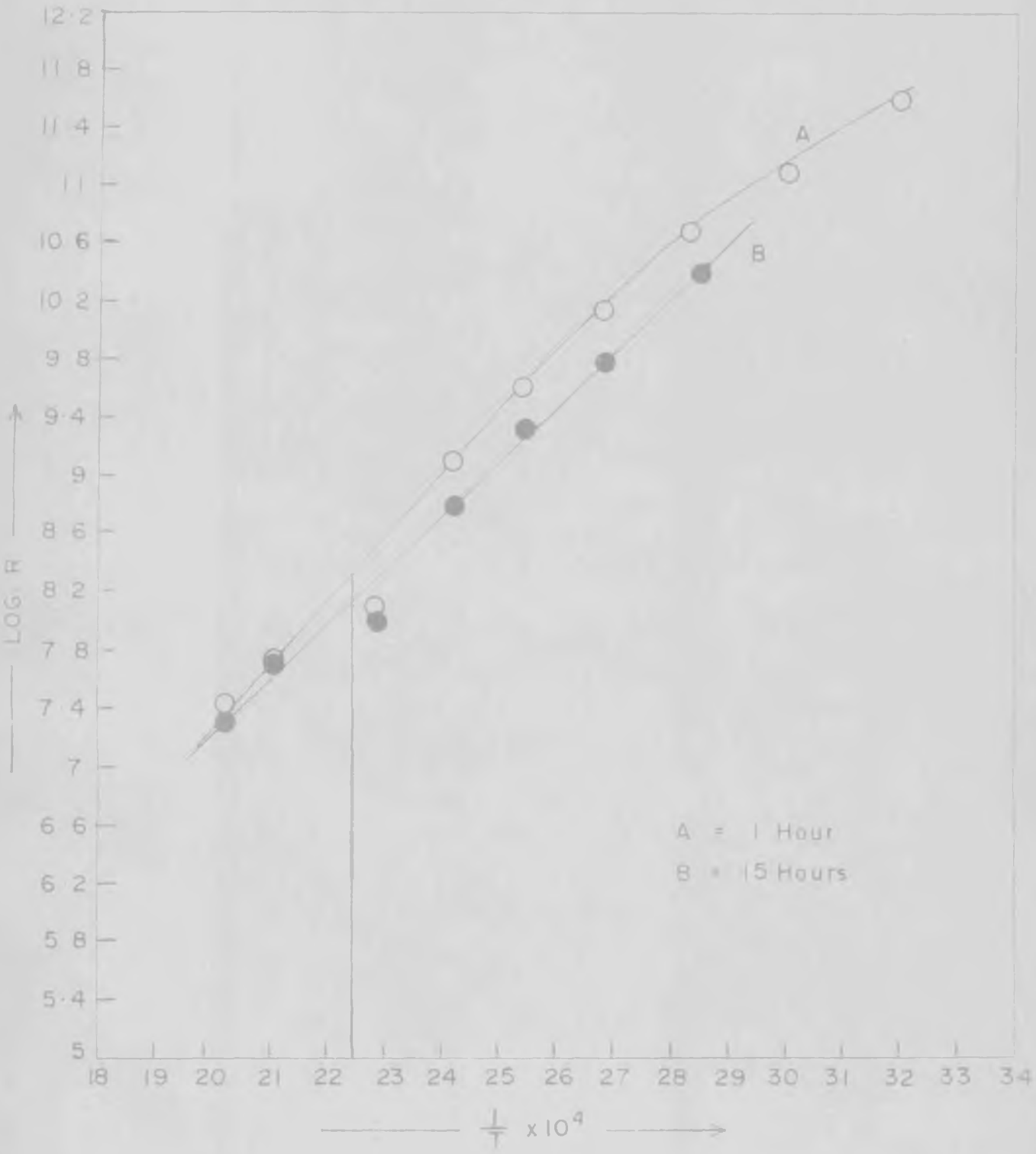

Fig 1.10 LOG R Vs $\frac{1}{T}$ PLOT FOR ZnO FILM. FILM PREPARED BY HEATING $Zn(OH)_2$ FILM AT 140°C FOR 1 Hr & 15 Hrs.

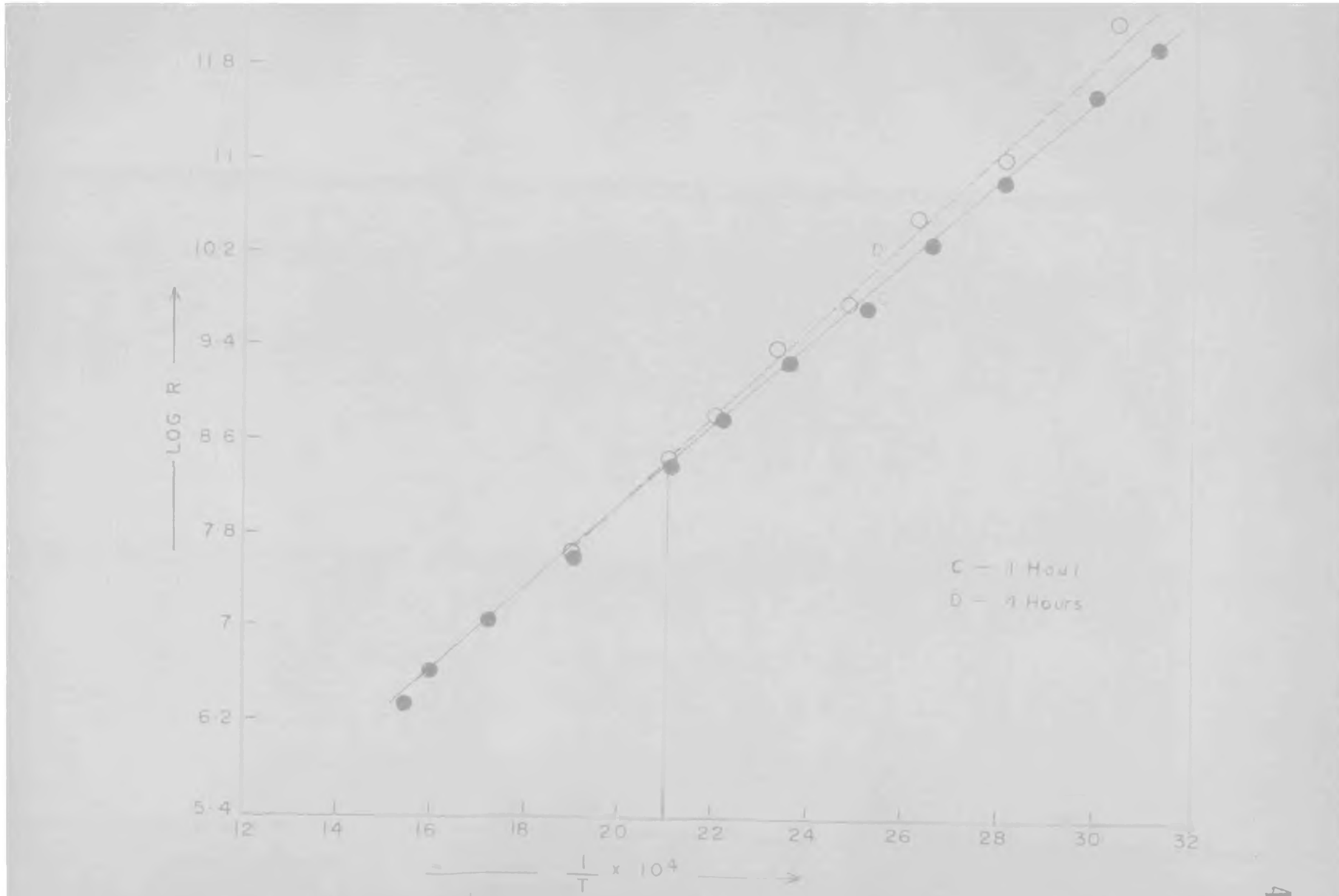

Fig 1.11 LOG R Vs $\frac{1}{T}$ PLOT FOR ZnO FILM PREPARED BY HEATING $Zn(OH)_2$ FILM AT 340°C FOR 1 Hr & 4 Hrs

heated at 340°C for 1 hour (C) and 4 hours (D) respectively.

All the graphs have the straight line nature which shows that $R = R_o \exp -\Delta E/kT$. The activation energy values ΔE in ev, are calculated from the formula

$$\Delta E = \frac{k(\log R_1 - \log R_2)}{[1/T_1 - 1/T_2]}$$

Fig. 1.12 shows the log R vs 1/T plot for the film previously heated at 450°C. The graph shows two slopes; one in the range 30-80°C and the other above 80°C.

The Table 1 gives the calculated activation energies for films heat treated at different temperatures.

Table 1

Film treatment	140°C 1 hour low temp.	15 hrs.	340°C 1 hour	4 hrs.	450°C 1 hour
Activation energy	0.87	0.7	0.73	0.73	0.24, 0.79

For all these samples, resistance values are reversible with respect to temperature.

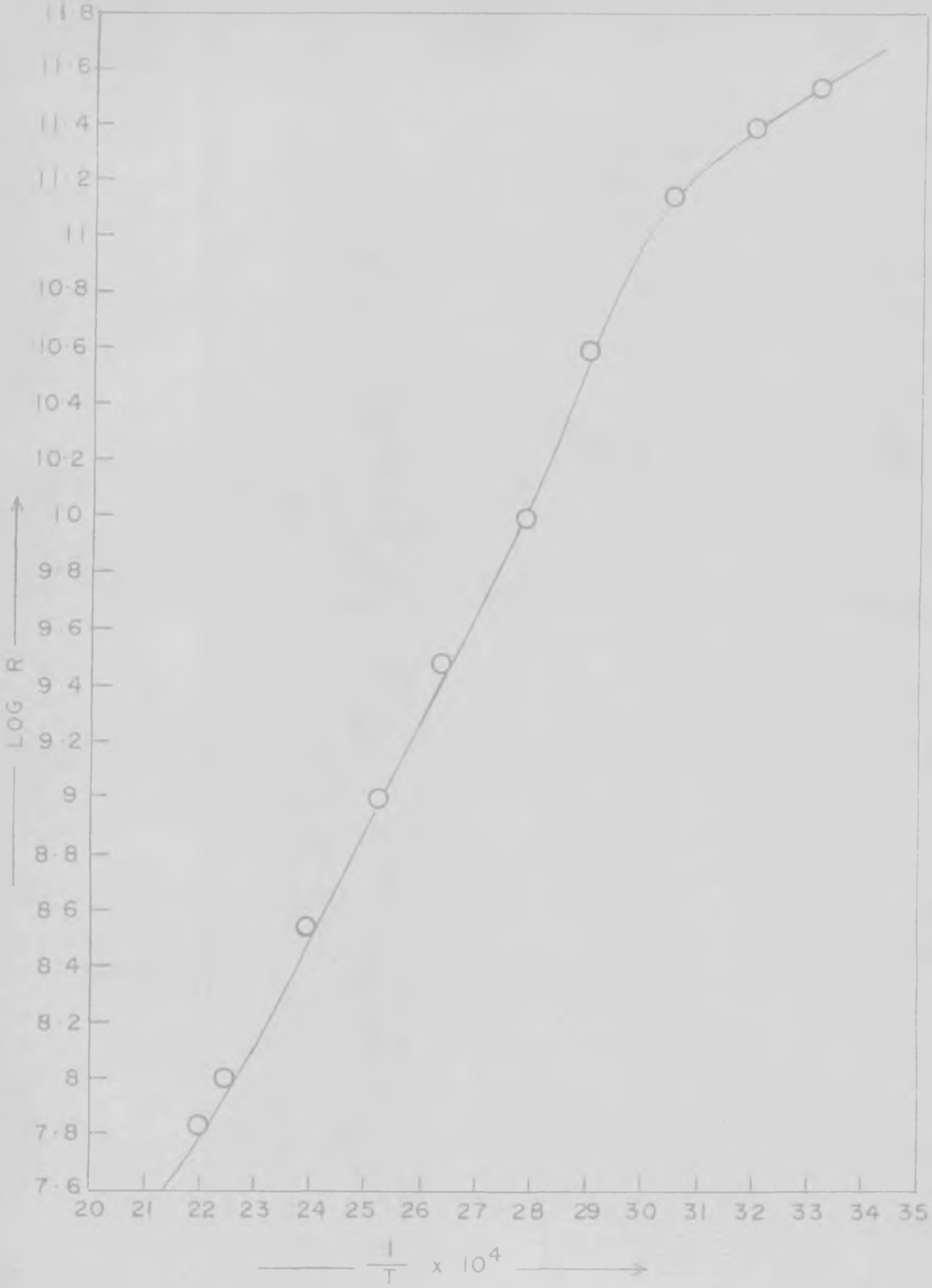

Fig 1·12 LOG R Vs $\frac{1}{T}$ PLOT FOR ZnO FILM

FILM PREPARED BY HEATING $Zn(OH)_2$ FILM AT 450°C FOR 1 HOUR

No effect of ambient gases or vacuum on the nature of the plots of log R vs 1/T was observed for these films under our experimental conditions.

For films heated at 850°C, the log R-1/T curve are as shown in Fig. 1.13. Fig. 1.14 gives log R-1/T plot for the film heated at 1000°C and quickly cooled to room temperature. Fig. 1.15 shows log R vs 1/T (quenched) curve for the film heated at 1000°C and slowly cooled in air to room temperature.

The features of the curves are as follows:

(1) There is a steady drop in the resistance upto approx. 150°C.

(2) There is a sharp fall in resistance after the initial steady drop which extends upto approx. 250°C.

(3) After the minimum in the resistance around 250°C, the resistance rises.

(4) The resistance reaches a maximum at 350°C. This is followed by a sharp fall in resistance which is observed upto 500°C, the maximum temperature of study.

The temperatures at which the maximum and minimum are obtained vary from sample to sample.

While cooling the sample, the maximum and minimum in the curve are not observed. Once the sample is heated upto 500°C and cooled to room temperature, the log R-1/T plot does not show any maximum or minimum (Fig. 1.15).

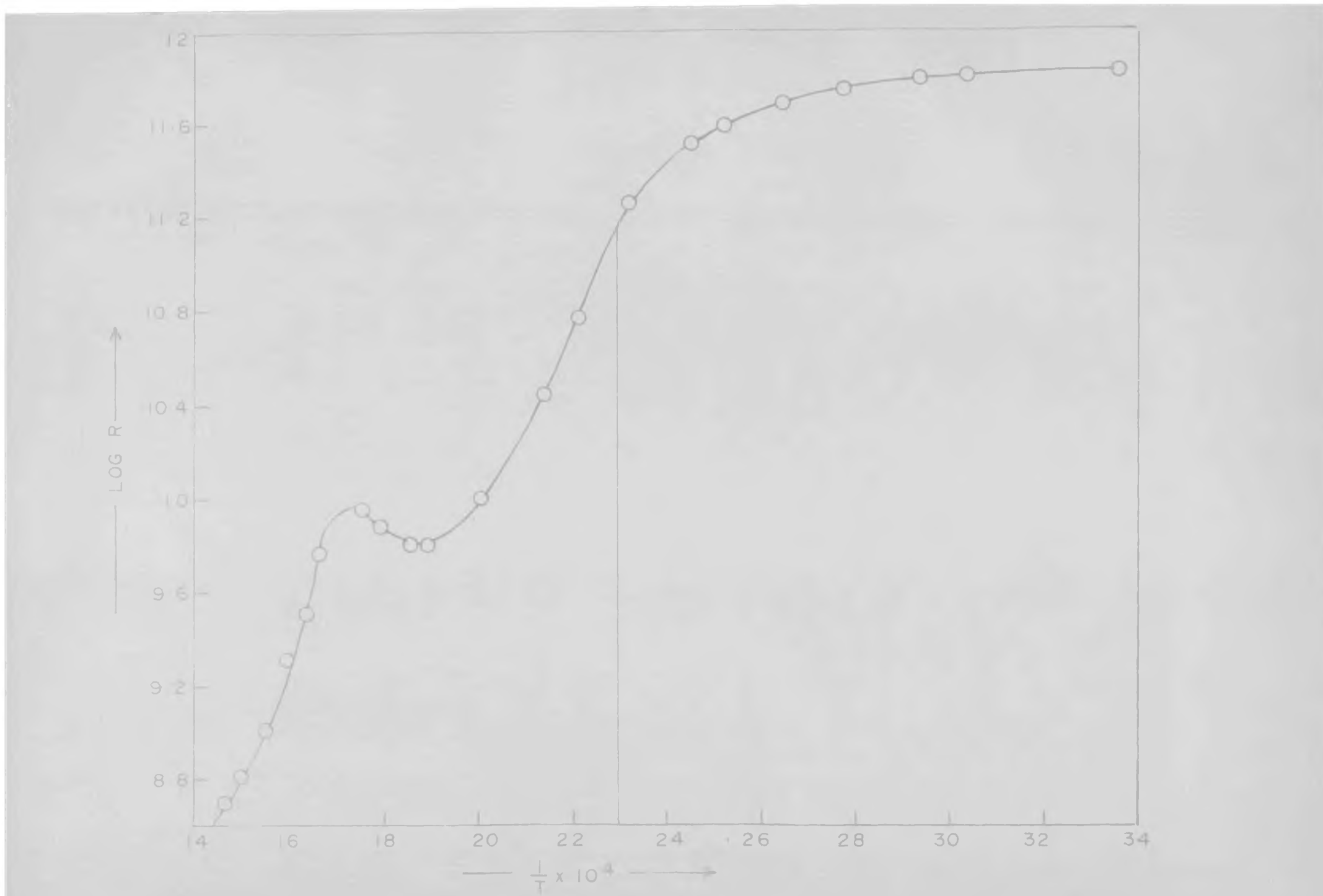

LOG R Vs $\frac{1}{T}$ PLOT FOR ZnO FILM

Fig 3.13 FILM PREPARED BY HEATING $Zn(OH)_2$ FILM AT 850°C FOR 1 HOUR

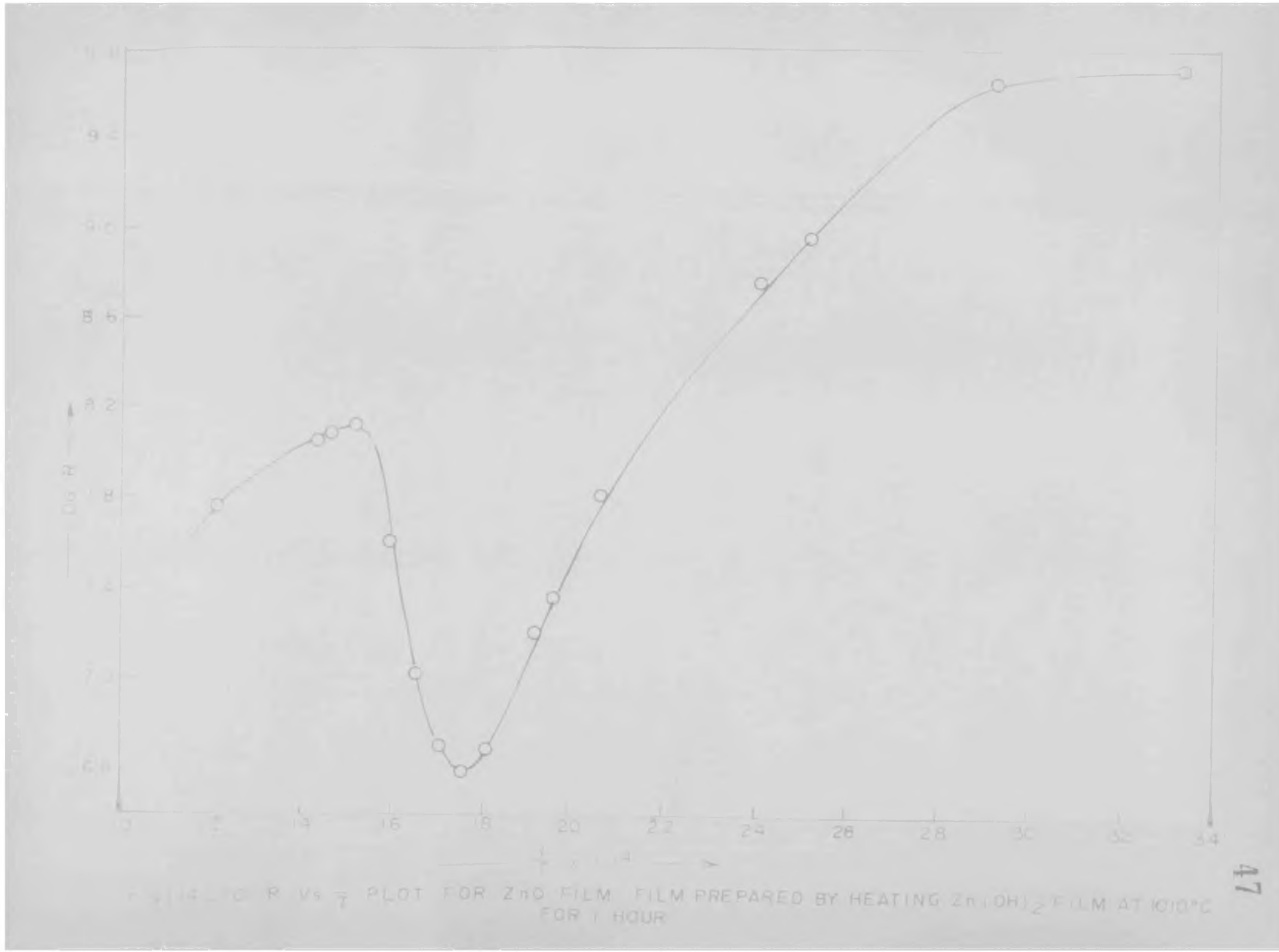

FIG. 4.10 R Vs $\frac{1}{T}$ PLOT FOR ZnO FILM FILM PREPARED BY HEATING $Zn(OH)_2$ FILM AT 1010°C FOR 1 HOUR

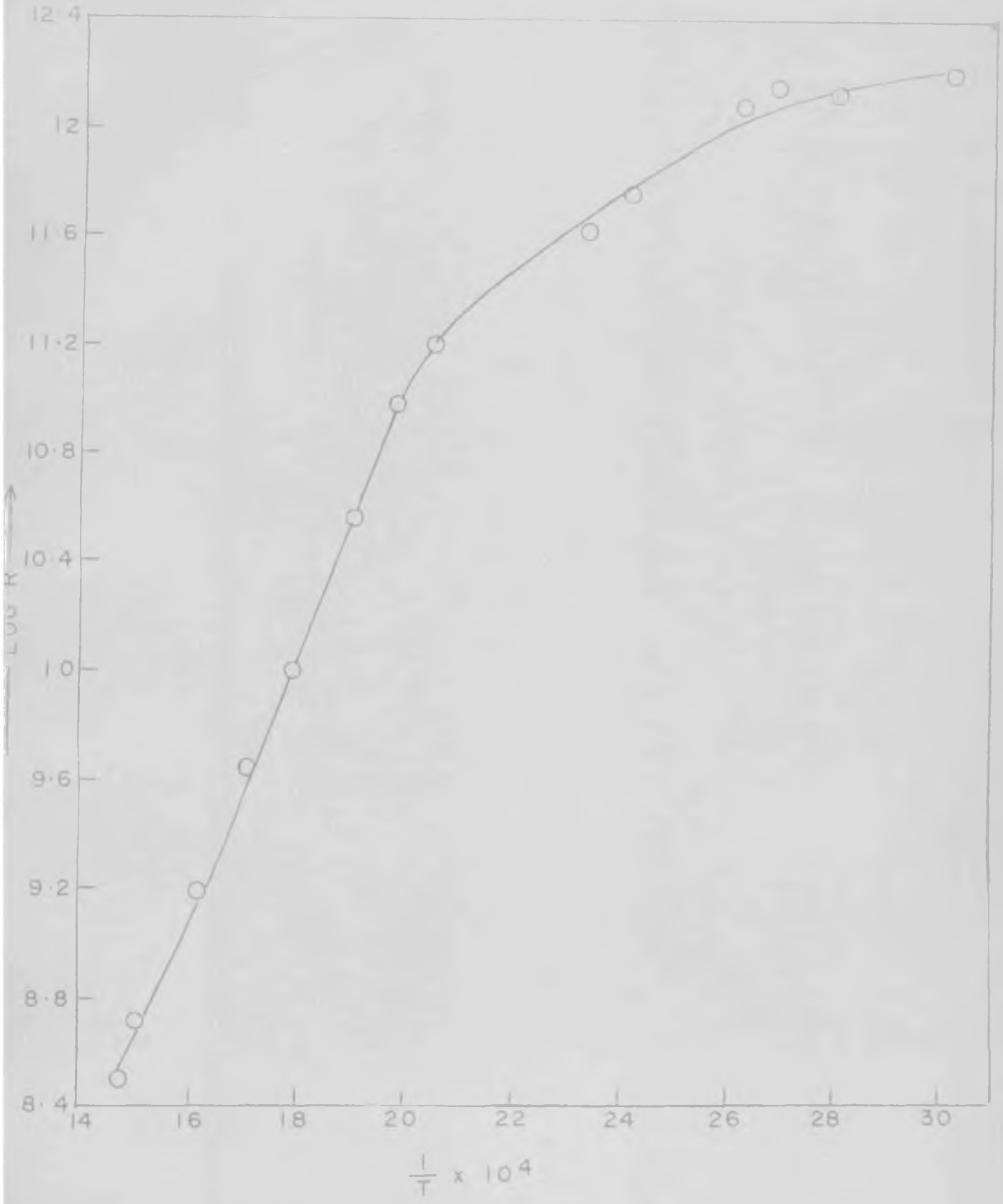

Fig I 15 LOG R Vs $\frac{1}{T}$ PLOT FOR ZnO FILM WHILE COOLING FROM 500°C TO ROOM TEMP.

The sample, for which the maximum and minimum have disappeared after heating it once to 500°C does not get its original state (showing maximum and minimum in log R-1/T plot) by heating it, in the atmospheres of oxygen, hydrogen, air, nitrogen or vacuum. If however the sample is wetted by water, dried and tested, then the maximum and minimum in log R-1/T curve reappear. This has been shown in the curve in Fig. 1.16.

The maximum and the minimum in the curve are not observed if the sample is tested in the atmosphere other than air. Oxygen, hydrogen, vacuum, have been tried for such experiments. Fig. 1.17 shows log R-1/T plot for the fresh sample heated in vacuum.

Fig. 1.18 gives the cycle, heating-cooling-heating to 500°C for a fresh sample. Observations are:

(1) During the first heating, maximum and minimum occur in log R-1/T plot.

(2) Cooling does not show any extrema.

(3) Second heating also does not show maximum and minimum.

(4) For cooling and second heating the curve is more or less reversible.

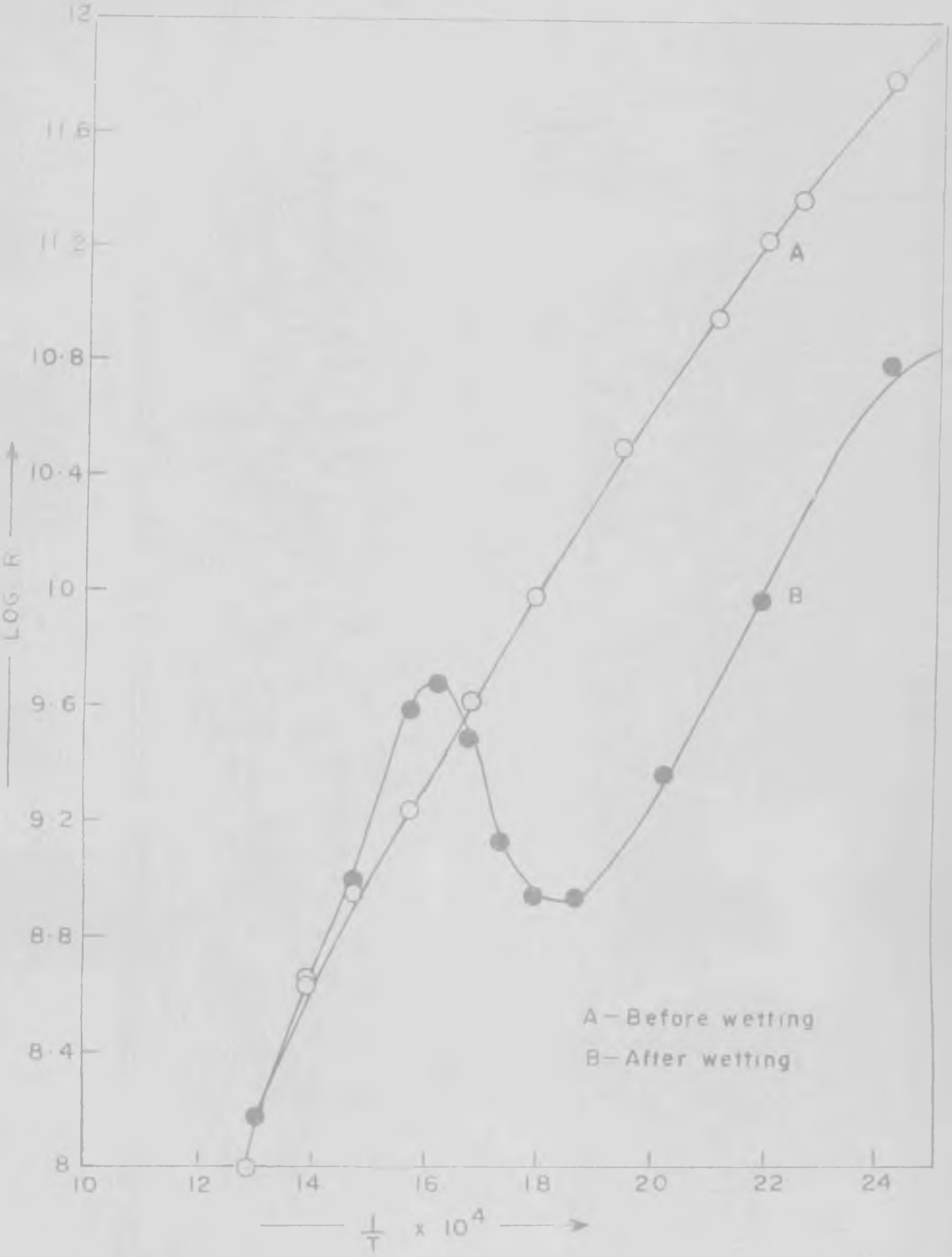

Fig 1.16 RECOVERY OF THE CONDUCTIVITY CHARACTARISTICS OF ZnO FILM ON 'WETTING' WITH WATER

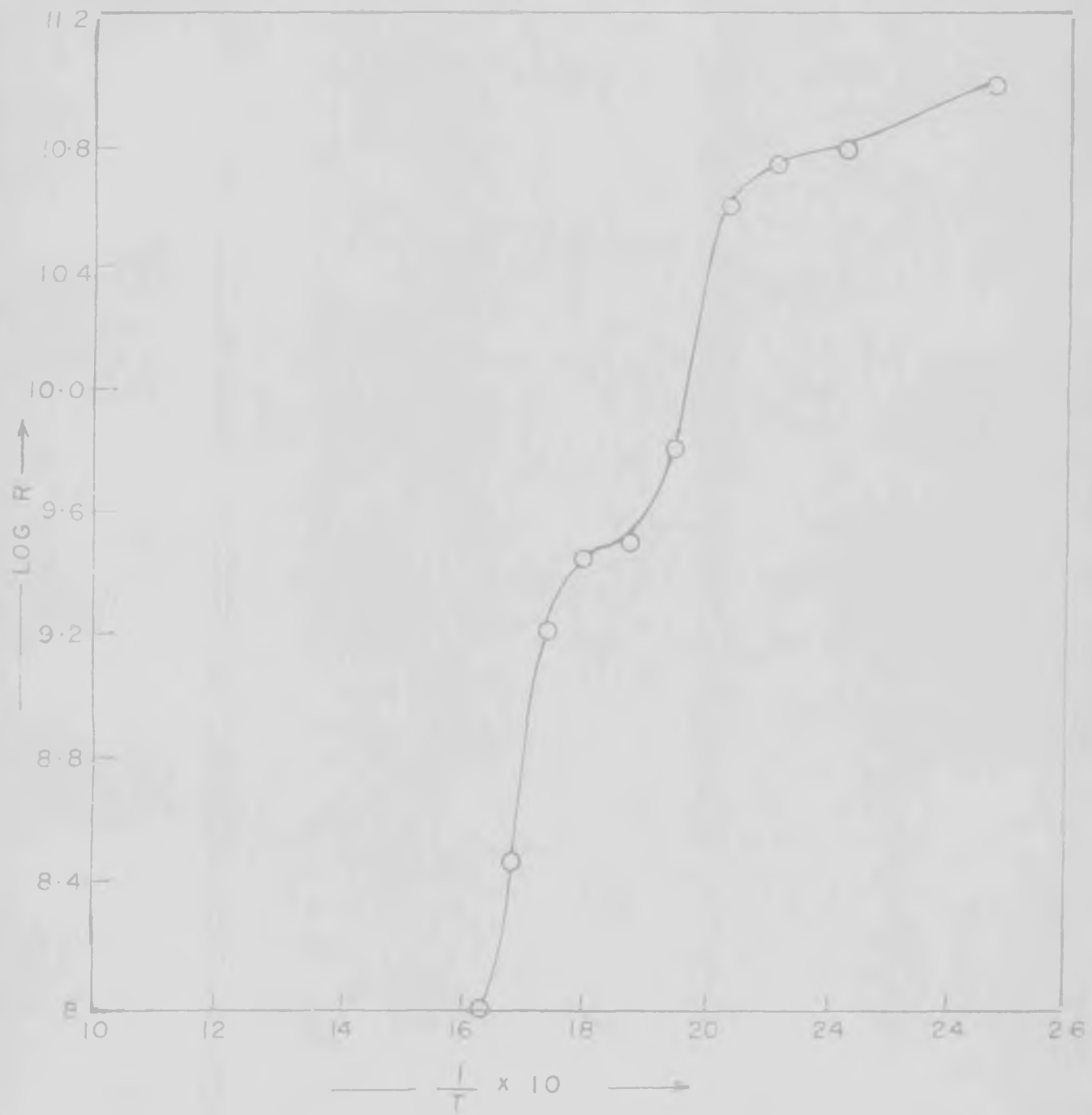

Fig 1·17 LOG R Vs $\frac{1}{T}$ PLOT FOR THE FRESH ZnO SAMPLE IN VACUUM

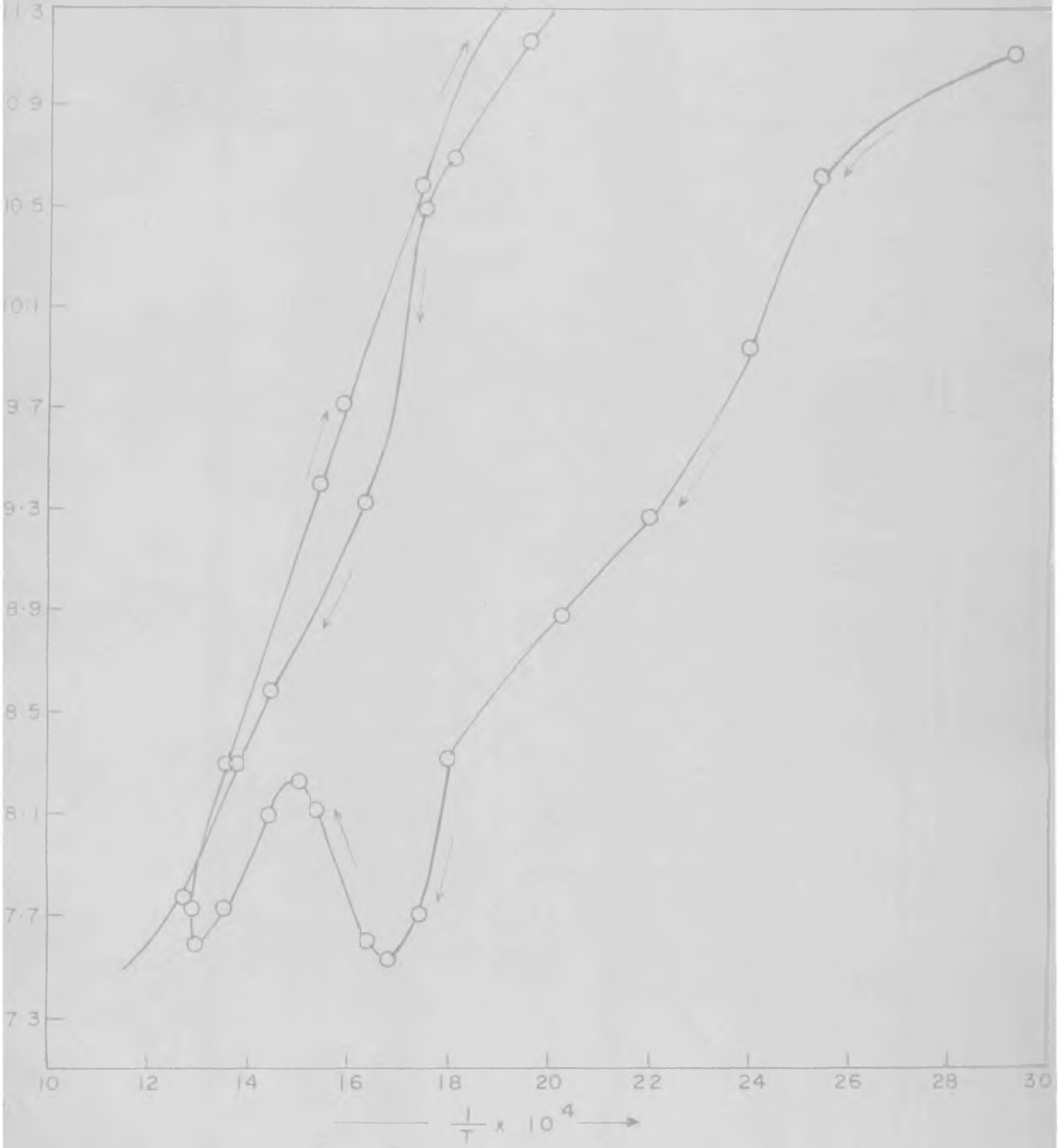

Fig 1·18 LOG R Vs $\frac{1}{T}$ PLOT FOR ZnO FILM(Fresh) HEATING–COOLING–HEATING CYCLE

Table II gives the activation energies obtained for the films heated at 1000°C and 850°C.

Table II

Activation energy values for films showing maximum and minimum in log R vs 1/T curve

Film prepared by heating at		ΔE	
		25°C to 250°C	300°C to 500°C
1st heating	850°C	0.415	1.05
	1000°C	0.54	0.65
2nd heating	850°C	0.12	0.89
	1000°C	0.28	1.037

An attempt to measure the thermoelectric power failed because of the high resistance of the films. Very low values of thermoelectric voltage were always mixed up with the 'noise'. However, the measurements showed 'n' type behaviour for these films.

1.3.5. DEPENDENCE OF RESISTANCE ON AMBIENT GAS

Fig. 1.19 shows the log R-1/T plot for the zinc oxide film in hydrogen atmosphere. No maximum or minimum is observed in the curve. The fall in resistance upto 300°C is steady and

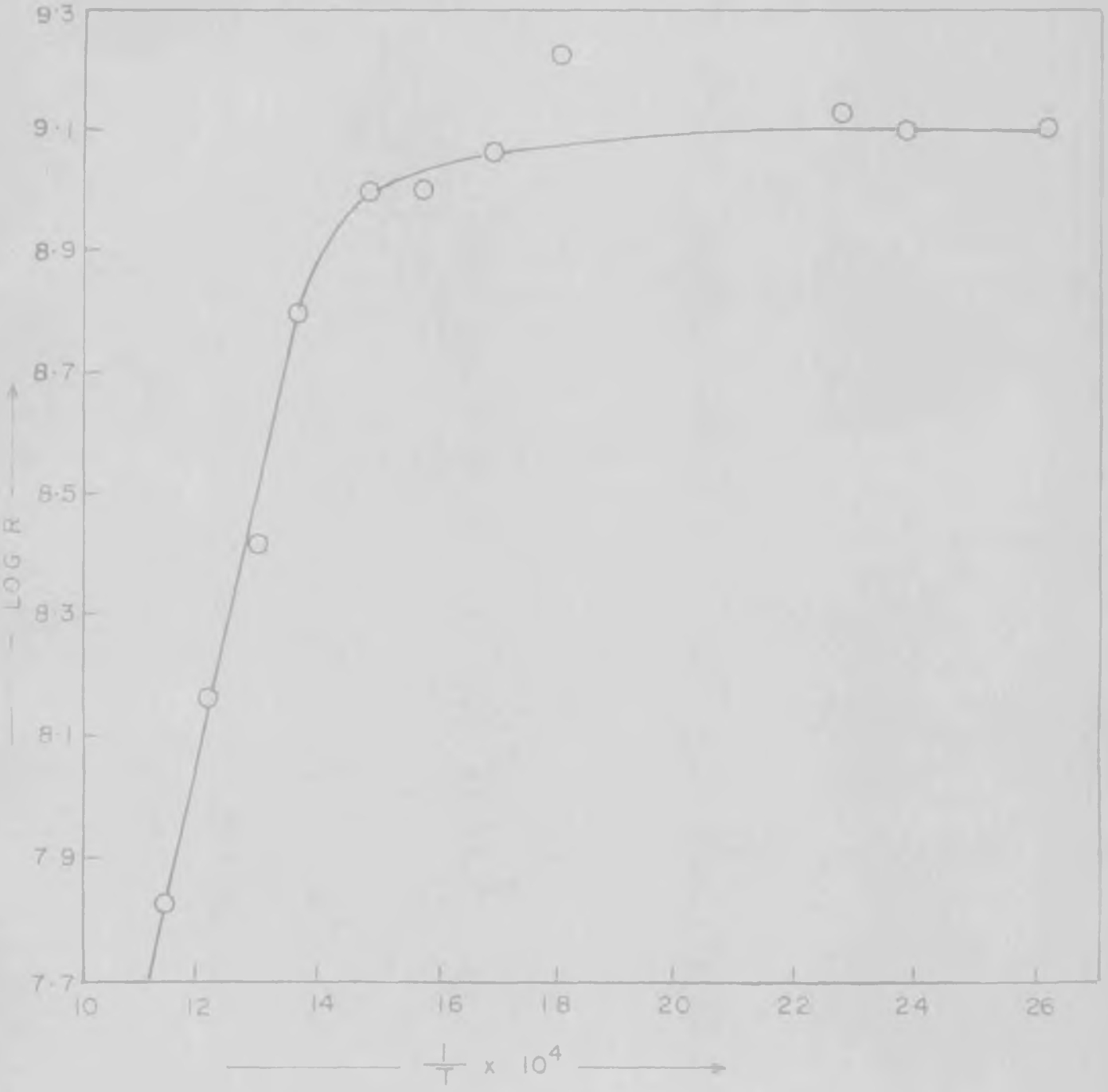

Fig 1·19. LOG R Vs $\frac{1}{T}$ PLOT FOR ZnO FILM IN HYDROGEN AMBIENT

above this temperature it is very steep. The activation energy calculations give $\Delta E = 0.794$ in the temperature range studied.

We have studied the pressure dependence of oxygen on the resistance of these films by recording the resistance at different oxygen pressures as shown in Fig. 1.21.

If we assume that the relationship $R = k\, p_{O_2}^{-1/m}$ is true, then as pressure increases, resistance will also increase; which can be observed in the curve of log R - log p_{O_2}. The slope will give the value of 1/m.

Observed values of m at different temperatures are:

T	m
200	6
300	3
400	3

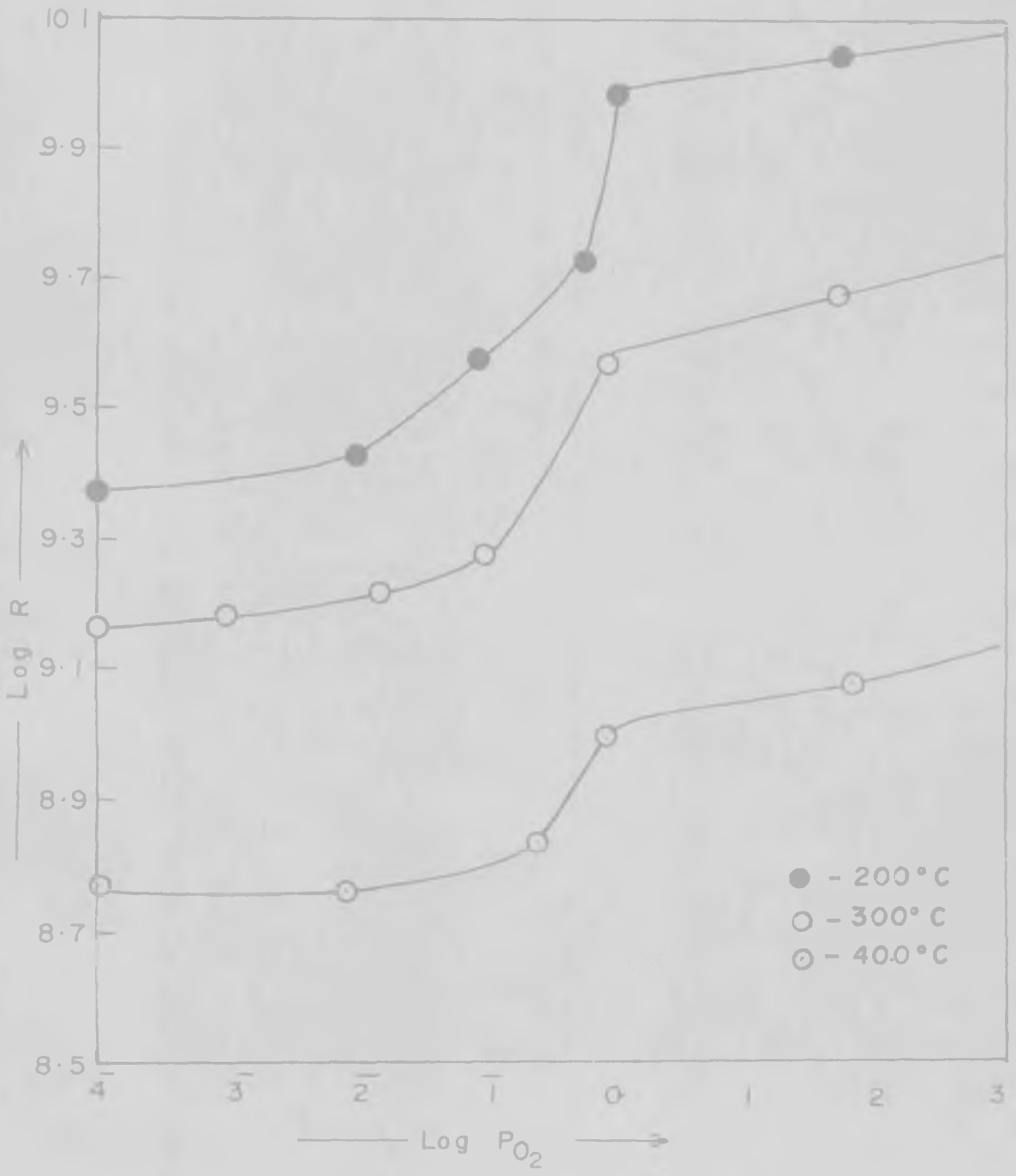

Fig I 20. LOG R Vs. LOG P_{O_2} PLOT FOR ZnO THIN FILM AT 200°, 300° and 400°C

CHAPTER - 4 - DISCUSSION

Some important new observations are as follows:

(1) The optical band gap for amorphous zinc oxide is more than that of the crystalline form. The absorption edge for the amorphous form is at 360 ± 5 nm while that for crystalline one is at 380 nm.

(2) The value of activation energy in different temperature zones is different for amorphous and crystalline zinc oxide:

Temp. °C	ΔE ev (amorphous)	ΔE(crystalline) ev
25-150	0.79 to 0.80	0.03 to 0.05
150 and above	-do-	0.8

(3) Whereas the conductivity of crystalline zinc oxide is strongly dependent on the ambient gases present, that of the amorphous form is not so, as far as our measurements indicate.

(4) The clear break and extrema shown in log R vs 1/T curves in case of fresh crystalline zinc oxide samples are absent in log R vs 1/T plots for the amorphous films (see Figs. 1.10, 1.11 and 1.12).

(5) The crystalline films prepared by the present new technique shows a minimum at 250°C and a maximum at 350°C which matches with those shown by the films prepared by the vacuum evaporation technique.

A fresh sample, studied after heating upto 500°C in air and cooling to room temperature, did not show the extrema in the log R vs 1/T curve (Fig. No. 1.14). However, it was found that just on wetting the sample with water and drying, it recovered its original conductivity characteristics i.e., it started showing the extrema in log R vs 1/T curve (Fig. No. 1.15).

In the only reported studies on noncrystalline zinc oxide thin films[44], the sputtering technique is used for sample preparation and the following properties have been studied: (a) influence of substrate temperature on film structure, (b) film crystallization, and (c) electrical conductivity.

The important results obtained are: (1) reactive sputtering of zinc metal on to a substrate maintained at low temperature in an oxygen-argon atmosphere forms noncrystalline zinc oxide films, (2) on heating at 75-100°C in vacuum or in air, crystallization of the films takes place, (3) optical absorption study shows that the band gap increases for the crystalline to noncrystalline transition, (4) the electrical conductivity for noncrystalline state is very low.

The work done on different amorphous materials by many workers[45] reveals that in general the optical band gap in the amorphous state is lower than the band gap in the corresponding crystalline form. The sharpness is lost in absorption vs wave length curve for the amorphous state as against the sharp edge

for crystalline form. Another observation shows that the density of the amorphous form is always less than that of the crystalline form.

In the present case, the films formed by heating at 850°C or above show the optical absorption edge at about 380 nm. This value is in agreement with that shown for the nearly stoichiometric zinc oxide single crystals. The amorphous samples prepared by heating at 340°C or 450°C show the optical absorption edge on the lower wavelength side of the spectrum. This result is in agreement with the result reported by Kingery et al.[44] on zinc oxide thin films. However, these results do not agree with the results by Kolomiets et al.[45] on amorphous As_2S_3 and As_2Se_3, which show that amorphous state optical band gap is lower than that of crystalline form.

The shift in the optical absorption edge to a lower wavelength side in our samples is small. The explanation given by Kingery et al.[44] may fit well to our observations. The lower density may decrease the dielectric constant resulting in the increased band gap. Such explanation does not require the hypothesis of a change in short-range order, but uses the general observation that the density of amorphous semiconductor is always less than that of the corresponding crystalline form. Denovan[46] and Clark[47], for example, have shown that the density of amorphous Ge is less than that of crystalline Ge.

The theories developed for the energy states in noncrystalline solids by Gubenov[48], Mott and others[49], indicate that in these solids also the band structure is retained though it may differ from the band structure of crystalline solids in some respects.

Fig. 121 shows the difference in the structure of band for crystalline and amorphous state. The features of the amorphous band structure are the 'tails' of localised states in the forbidden gap. These tails may overlap as shown by Gabenov[48]. This change in the band diagram helps in explaining many properties of amorphous semiconductors such as diffused band edge, intrinsic conductivity character, etc.

The crystalline zinc oxide thin films show a very low value of activation energy (0.03 to 0.05 ev) for the temperature range 25-150°C. This has been accepted as due to the ionization of excess interstitial zinc in the lattice. From 150°C to 500°C, a straight line portion in log R vs 1/T curve (Fig. 1.14) gives the value of the activation energy as 0.8 ev. This is in agreement with the value expected for the oxygen level in the forbidden gap. Film heated at 450°C also shows similar straight lines in log R vs 1/T curve.

Noncrystalline films, however, do not show the activation energy of 0.03 to 0.05 ev in the temperature range 25°C to 500°C,

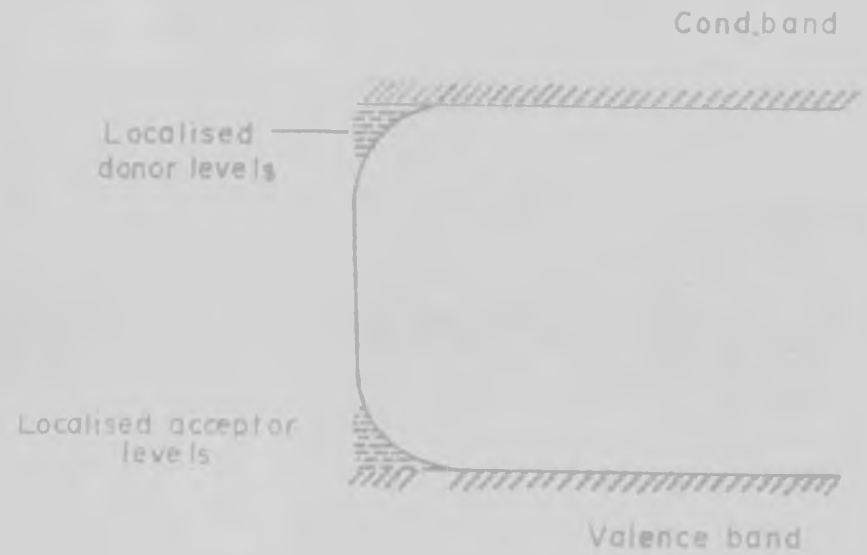

AMORPHOUS STATE (a)

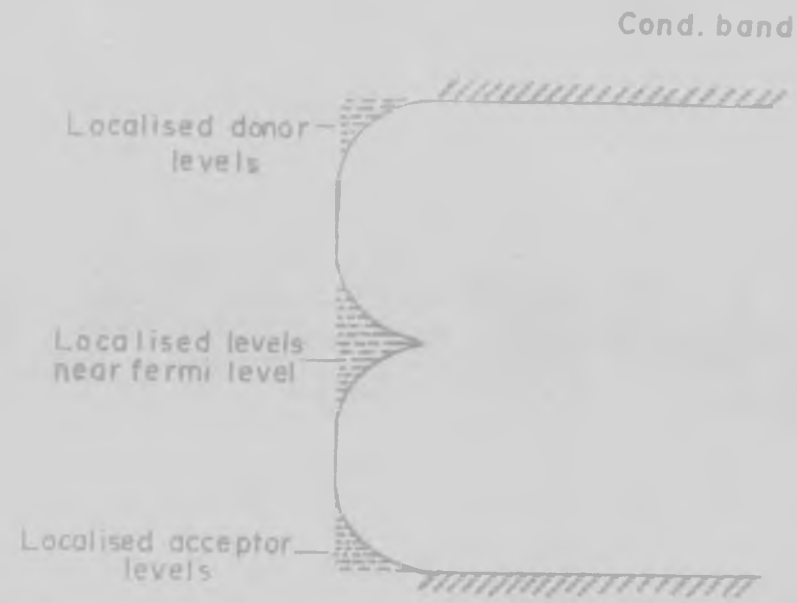

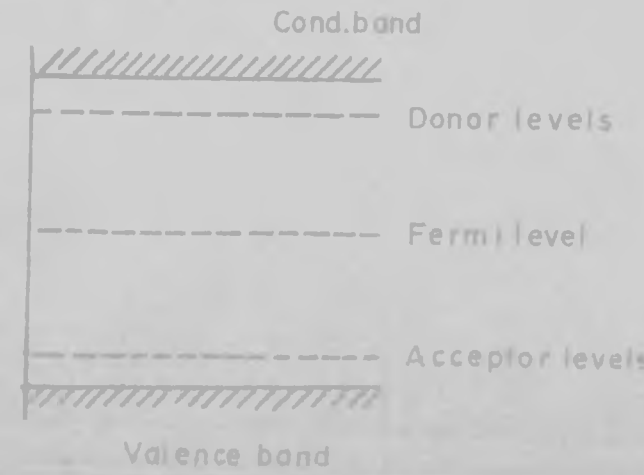

CRYSTALLINE STATE (b)

Fig 1.21

possibly due to the fact that the low temperatures used in the preparation of these films (140°C, 340°C) are not expected to remove any oxygen from zinc oxide, except the adsorbed oxygen. The composition is, therefore, likely to be nearly stoichiometric without any excess zinc.

The straight line in log R vs 1/T curve corresponding to the activation energy of 0.8 ev in crystalline zinc oxide film is shown from 150°C-500°C, whereas in noncrystalline films it is shown right from room temperature to 250°C. (Figs. 1.10, 1.11).

It may be emphasised that in cases where two energy levels contribute to the carriers responsible for conduction, the temperature at which the transition from low to high activation energy takes place depends on the relative density of states at these two levels. The fact that the amorphous variety shows the high activation energy right from room temperature onwards, shows that the transition has taken at a lower temperature.

This should mean that (1) either the density of low activation energy states is less in amorphous state as compared to the crystalline, or (2) the density of high energy states is more. In the former case, the resistance of crystalline and nonerystalline films would be of the same order at higher temperature at which high activation energy levels dominate. The latter possibility should lead to a lower resistance for amorphous material at the higher temperatures.

Since in the higher temperature region the resistance of the amorphous form is lower, it shows that the density in low lying level (high activation energy) is more in the amorphous than the crystalline state. If this energy level is due to adsorbed oxygen then it is possible that this may dominate the properties of amorphous zinc oxide thin films with higher surface area.

The initial resistance of crystalline and noncrystalline zinc oxide films is of the same order at room temperature. This is contrary to the generally accepted observation of decrease in resistance from the noncrystalline to crystalline transition. Kingery et al.[44] observed such change in zinc oxide at about 95°C in zinc oxide films. We explain this opposite observation in our samples as due to the effect of moisture which reduces the contact resistance in noncrystalline state which is the major factor for higher resistance of the material in that state. Oster and Yamamoto[50] have also explained their results of enhanced conductivity due to water vapour in photoconductivity studies.

Another possibility would be on the lines suggested by Gubanov[48] that there is a disappearance of impurity levels in the noncrystalline semiconductors. This explains the absence of 0.03 to 0.05 ev levels. The levels corresponding to the activation energy of 0.8 ev may be due to structural defects and short range order fluctuations. Results of Kolomiets et al.[51]

for $Tl_2SeAs_2Te_3$ and As_2Se_3 glasses and Chaudhari et al.[52] for amorphous $3As_2Se_3.2Sb_2Se_3$ films also show evidance of such trap levels. Absence of long range ordering produces tailing of the band edges by which 0.03 ev levels may disappear. This explanation is consistent with the generally accepted belief that oxygen levels would be present only if excess zinc is effective as an adsorption site. Also, it is observed that resistance is not dependent on ambient conditions. This agrees with the explanation given above. It is difficult to predict the exact cause of the change in the activation levels in the band gap when the change from nonerystalline to erystalline state occurs from the data available. However, the former explanation is more acceptable as the value of the activation energy of 0.8 ev in noncrystalline films matches with the level of adsorbed oxygen and this may not be a mere coincidence.

The presence of extrema in log R vs 1/T curve has been studied previously by Stöckmann et al.[53] on thin films of zinc oxide, Arghiropoulos et al.[42] on zinc oxide pellets and Prafulla Chandra et al.[54] in case of surface study of ZnO single crystals. The later two papers give the explanation of disappearance of extrema during the second heating of the sample and only Prafulla Chandra et al.[54] explained the reappearance of extrema.

Morrisson[21] explained Stöckmann's[53] results as follows:

The level at the depth of 0.8 ev below the bottom of the conduction band designated as O^{--} levels, which correspond to the

energy required for dissociating an electron from O^{--}_{ads} giving rise to O^{-}_{ads}. There is another level at the depth of 2.4 ev, designated as O^{-} which corresponds to the dissociation of an electron from O^{-}_{ads} giving rise to O_{ads} and an electron in the conduction band. At room temperature, electrons are available from the excess Zn donors present interstitially. Upto 250°C, the electrons cannot reach the adsorbed oxygen at the surface. At 250°C, the number of electrons available for conduction and the number consumed due to chemisorption of O^{-} species is equal. Above 250°C, O^{-} chemisorption dominates and consumes more electrons than available for conduction and thus the resistance increases. This continues upto 450°C where desorption starts making available more electrons for conduction and the resistance again decreases showing a maximum in the log R vs 1/T plot.

Arghiropoulos et al.[42] observed extrema in ZnO pellets and explained the phenomenon as arising due to the interplay of two opposing factors:

(1) The liberation of electrons due to thermal ionization of Zn interstitials. At the same time, Zn interstitials themselve migrate to the surface due to the influence of strong electric field present there.

(2) Electron consumption due to chemisorption.

Prafulla Chandra[64] studied the surface conductivity of single crystals and found the presence of the same type of

the maximum and minimum in log R vs 1/T curve. The explanation given was based on the following reactions:

$$O^-_{ads} \longleftrightarrow 1/2\ O_2 + e^- \qquad \ldots 1$$

$$Zn_i + O^-_{ads} \longrightarrow (Zn^{++}O^{--})_{surface} + e^- \qquad \ldots 2$$

$$Zn_i^{+} \longrightarrow Zn_i^{++} + e^- \qquad \ldots 3$$

Finally, they gave the relation:

$$n^2 = B \exp\left[- \frac{E_1 + E_3 - E_2}{kT} \right]$$

where n = number of electrons available for conduction,

E_1, E_2, E_3 = corresponding enthalpy changes for reactions 1, 2 and 3,

k = Boltzmann constant,

T = Absolute temperature.

When $E_1 + E_3 - E_2$ is positive, minimum in log R vs 1/T and $E_1 + E_3 - E_2$ is negative, maximum in the curve is obtained. In the sample once heated at 500°C, extrema are not shown because reaction 3 is absent, due to the formation of stoichiometric ZnO layer at the surface during the previous cycle. When this layer is removed by etching, fresh surface again shows original characteristics with maximum and minimum in log R vs 1/T curve.

Morrison's[21] theory is not able to explain the non-cyclic nature. In other words, the disappearance of the maximum and minimum in the sample, once heated to 500°C, is not explained, because all the reactions involved are reversible.

Arghiropoulos[42] et al. have not considered the oxygen state adsorbed at the surface. It has been an agreed fact that O_2 is adsorbed on zinc oxide in two different states; one stable at low temperatures and reversible, and the other stable at high temperatures above 200°C but irreversibly adsorbed. Also, the authors have not attempted to find out the treatment by which the sample not showing the extrema in log R vs 1/T curve, starts showing the maximum and the minimum.

As described earlier, our results show that the sample not showing the extrema, if wetted by water, starts showing a maximum and a minimum in log R vs 1/T curve. Prafulla Chandra et al.[54] have shown how the top surface layer is the determining factor for the extrema in the log R vs $1/T$ curve. We consider, the state of oxygen, O^- or O^{--} at the surface determines the nature of log R vs $1/T$ curve. This also explains the observation by Prafulla Chandra et al.[54], i.e. how the crystal, not showing the extrema in conductivity curve, starts showing the same after it is etched and the top surface removed.

For interpreting the maximum and the minimum, we suggest the following mechanism based on the model proposed by Barry and Stone.[40]

The absorption desorption of oxygen shows that two types of adsorbed species are present on zinc oxide surfaces. Morrisson has suggested that O^{--} state is stable at lower temperatures upto 200°C and O^{-} state is stable at higher temperatures. Barry and Stone[40] suggest that O^{-} is stable below 200°C and O^{--} above 200°C. All workers agree that the state stable at lower temperatures is reversible while the other is not.

When the oxygen is adsorbed at the surface of zinc oxide, it takes up electrons forming negatively charged layer, at the surface. This creates a barrier for electrons to reach oxygen in equilibrium with the surface.

At any temperature, this barrier height will increase with increasing number of oxygen atoms getting adsorbed on the surface and at equilibrium no electrons would have enough energy to cross this barrier. This is called as "pinch off" effect by Morrisson[21].

For the film heated at 850°C or above and quenched to room temperature, zinc interstitials are formed. The activation energy for the ionization of these donors is of the order of

0.05 ev, therefore, at room temperature the reaction

$$Zn_i \longrightarrow Zn_i^+ + e^- \qquad \ldots 1$$

will take place. As the temperature increases, more Zn_i will ionize giving free electrons in the conduction band. Since the number of Zn_i is very large, the reaction

$$1/2\ O_2 + e^- \longrightarrow O^- \qquad \ldots 2$$

will not affect the number of electrons in the conduction band and the resistance will reduce. This continues upto 250°C where the reactions:

$$O^- \longrightarrow 1/2\ O_2 + e^- \qquad \ldots 3$$

$$\text{and} \quad O^- + e^- \longrightarrow O^{--} \qquad \ldots 4$$

start taking part in the mechanism. Since we record the resistance at equilibrium, only the reaction 4 will contribute at this stage. When reaction 4 dominates and just overcomes the effect of reaction 1, minimum in the curve is obtained and resistance starts increasing. At temperatures above 350°C, the following reactions should be considered:

$$Zn_i^+ \longrightarrow Zn_i^{++} + e^- \qquad \ldots 5$$

$$Zn^{++} + O^{--} \longrightarrow (Zn^{++}O^{--})_{\text{lattice}} \qquad \ldots 6$$

$$O^{--} \longrightarrow 1/2\ O_2 + 2e^-_{(\text{desorption})}. \qquad \ldots 7$$

These reactions make more electrons available and hence dominate

reaction 4 through a maximum around 370°C. Then the resistance decreases due to reactions 5, 6 and 7 upto 500°C.

It may be noted that the reaction 6 is very slow. The electrical field created at the surface by negatively charged oxygen ions (of the order of 10^6 v/cm)[42] helps the diffusion of interstitial zinc, from bulk to the surface. This reaction will be faster than reaction 6 so that there will always be excess zinc present at the surface.

While cooling, all except the process $O^- + e^- \rightarrow O^{--}$ would reverse. Hence the oxygen at the surface at room temperature will be in O^{--} state rather than O^-, which was the starting state for the fresh sample. The increase in resistance with increasing temperature in the range 270°C to 350°C is due to the reaction (4) i.e. $O^- + e^- \rightarrow O^{--}$.

This reaction is the cause of the maximum and the minimum in the log R vs 1/T curve which will be absent once the sample is heated upto 500°C in air. This is also shown in the heating-cooling-heating cycle as shown in Fig. 1.16. The room temperature resistance in the heated sample is very much higher than the corresponding resistance for the fresh sample. Now when the film is wetted, the following reaction may take place:

$$O^{--} + H_2O \longrightarrow (H_2O_2)^- + e^- \qquad \ldots 8$$

This shows how the resistance is decreased for the film wetted and dried as shown in Fig. 1.15.

During the heating process, initially the water gets lost through the reaction

$$(H_2O_2)^- \longrightarrow H_2O + O^-$$

leaving the adsorbed species, which in other words, brings the sample back to the original state. Now onwards, all other processes will be the same as described earlier showing maximum and minimum in log R vs 1/T plot.

The possibility of the formation of $(H_2O_2)^-$ species has been predicted in photoconductivity experiments. The observation made by Prafulla Chandra et al.[54] that by removing the top layer of the crystal by etching reproduces the extrema in the conductivity curve can be explained by this model. Top layer of the crystal heated once at 500°C in air will have the oxygen in the O^{--} state at the surface. When this layer is removed oxygen will be adsorbed at room temperature in O^- state; which is the necessary condition for extrema properties in log R vs 1/T curve. The support to the existence of O^- state at lower temperatures and O^{--} at temperatures higher than 200°C is obtained from A. M. Peers[55], Glemza and Kockes[56], Seedat and Kwan[57], etc. Peers suggests direct conversion of O^- to O^{--} through $O^- + e^- \longrightarrow O^{--}$ at 200°C while Glemza and Kokes[56]

give indirect reaction as

$$Zn_i + O_s^- \longrightarrow Zn_i^{++}O^{--} + e^-.$$

Kwan et al.[57] gave the evidence for the reactions

$$O_2^- + e^- \longrightarrow 2O^-$$

$$O^- + e^- \longrightarrow O^{--}$$

from ESR spectra. Recently, such transformations on other oxides like Ti^{3+} have also been reported from ESR studies[58].

According to the model proposed by Barry and Stone[40], at room temperature ZnO having excess Zn will have chemisorbed oxygen in the state O_2^- or O^- and at higher temperatures (above 200°C) O^{--} state will be present. O^- ions will act as the active centres for hydrogen chemisorption.

To explain the effect of hydrogen ambient on the conductivity of zinc oxide films, two observations should be considered (Fig. No. 1.17):

(1) Upto 250°C, there is no change in the nature of log R vs 1/T plot from the one obtained in absence of hydrogen.

(2) Above 250°C, there is a steep fall in resistance. No maximum or minimum in the log R vs 1/T curve is observed.

At room temperature there will be an equilibrium between the free electrons in the conduction band and bound by the

chemisorbed oxygen, represented by the reactions:

$$Zn_i \longrightarrow Zn_i^+ + e^-$$

$$1/2\ O_2 + e^- \longrightarrow O^-$$

or

$$O_2 + e^- \longrightarrow O_2^-.$$

Since the O^- sites will take up hydrogen by the reaction $O^- + 1/2\ H_2 \quad OH^-$, the equilibrium with respect to electrons is not disturbed. The number of electrons available for conduction is not altered. This will continue upto 200°C, at which temperature some O^- sites are lost by desorption and the remaining by converting themselves into O^{--} sites

$$O^- \longrightarrow 1/2\ O_2 + e^- \qquad \ldots 3$$

$$O^- + e^- \longrightarrow O^{--} \qquad \ldots 4$$

Above 250°C, hydrogen adsorbed(chemically) will affect the conductivity since the reaction

$$O^{--} + 1/2\ H_2 \longrightarrow OH^- + e^-$$

takes place indicating additional electron given by the chemisorption of hydrogen. The energy of activation of 0.8 ev is in agreement with the value reported by Morrisson[21].

Apart from these reactions, we expect some reduction of ZnO, at least at the surface, to take place above 200°C producing

more excess of Zn at the surface which will contribute to the conductivity by the reaction

$$Zn_{lattice} \longrightarrow Zn^{+}_{lattice} + e^{-}.$$

The dependence of resistance on oxygen pressure as shown in Fig. No. 1.18 is similar to one obtained by Oster et al.[50] in zinc oxide pellets at room temperature. The films are sensitive to oxygen pressure around pressure of the order of 10^{-2} mm. of Hg.

These results are explained with the help of the model proposed by Barry and Stone[40]. At low temperatures, below 200°C, oxygen is chemisorbed as O^{-} and at higher temperatures it is chemisorbed as O^{--} that may be stabilised by the migration of excess zinc, at the surface.

We observe that the effect of oxygen pressure on the films at 300°C and 400°C is less than the effect observed at 200°C. This is in agreement with the conclusion by Kokes'[59] theory based on the model proposed by Barry et al.[40].

REFERENCES

REFERENCES

1. R. W. G. Wyckoff,
Crystal Structures, Interscience Publishers,
p. 111, 1960.

2. O. Fritsch,
Ann. Physik, 5(22), 375, 1936.

3. S. E. Harrison,
Univ. Penn. Tech. Rept. No. 3, 1952,
[Solid State Phys. Vol. 8).

4. S. E. Harrison,
Phys. Rev., 93, 52, 1954.

5. G. Heiland,
Z. Physik., 132, 354, 1952.
132, 367, 1952.
138, 459, 1954.
142, 415, 1955.
148, 15, 1957.

6. F. Stöckmann,
Z. Physik, 127, 563, 1950.

7. H. Rupprecht,
J. Phys. Chem. Solids, 6, 144, 1958.

8. G. Tischer,
Dissertation, Univ. of Erlangen, 1954.
Solid State Phys., 8, 248.
Academic Press, 1954.

9. S. R. Morrison and P. H. Miller(Jr.),
Tech. Report No.6, Univ. of Penn, 1962.

10. D. J. M. Bevan and J. S. Anderson,
Diss. Faraday Soc., 31, 219, 1961.

11. K. Intemann and F. Stöckmann,
Z. Physik, 131, 10, 1951.

12. W. Jander and W. Stamm,
Z. Anorg. u. allgem. Chem.,
Solid State Phys., Vol. 8, p. 253.

13. E. E. Hahn,
J. Appl. Phys., 22, 855, 1951.

14. H. Preier,
Z. Fuer. Naturforsch,
19 a (12), 1431, 1964.

15. R. Glemza and R. Kokes,
J. Phys. Chem., 66, 566, 1962.

16. E. Mollow,
Z. Physik, 138, 478, 1954.

17. P. H. Miller,
Phys. Rev., 60(12) 890, 1941.

18. C. A. Hogarth,
Phil. Mag., 7(39), 260, 1948.
Nature, 161, 60, 1948.
Z. Physik Chem.(Leipzig) 198, 30, 1951.

19. J. J. Lander and D. G. Thomas,
J. Chem. Phys., 25, 1136, 1956.

20. W. Ruppel, H. J. Gerritsen, A. Rose,
Helv. Physica Acta, 30, 495, 1957.

21. S. R. Morrison,
Adv. in Catalysis, Vol. VII, 258,
Academic Press Inc. Publishers, New York, N.Y. 1955.

22. H. J. Krusmayer,
Phys. Rev., 114, 655, 1959.

23. J. J. Lander,
J. Phys. Chem. of Solids,
15(3-4), 324, 1960.

24. R. Schulter, M. L. Jauton and P. Douzu,
Compt. Rend, 250, 506, 1960.

25. I. A. Myasnikov,
Zhur. Fiz. Khim., 31, 1721-30, 1957.

26. A. Cimino., E. Molinari and F. Cramarossa,
J. Catalysis, 2(4), 315, 1963.

27. H. Watanabe and M. Wada,
Jap. J. Appl. Phys., 4(12), 945, 1965.

28. B. Hoffmann,
Solid State Comm., 5(1), 61-63, 1967.

29. J. MacNobbs,
J. Phys. Chem. Solids, 28(2), 205-10, 1967.

30. G. Heiland, E. Mollow and F. Stöckmann,
Solid State Phys., 8, 282-285, Academic Press, 1959.

31. H. Weiss,
Z. Physik, 132, 335, 1952.

32. D. A. Melnik,
Phys. Rev., 94, 1438, 1954.

33. A. R. Hutson, R. J. Collins and D. G. Thomas,
Phys. Rev., 112(2), 288, 1958.

34. P. K. Kasai,
Phys. Rev., 130(3), 989, 1963.

35. T. J. Gray and P. Amigues,
Surface Science, 13(1), 209, 1969.

36. E. Mollow,
Reichsber. Physik, 1, 1, 1943.

37. C. Duval and M. de Clerk,
Anal. Chim.Acta, 5, 282, 1951.
Inorganic Thermogravimetric Analysis,
Elsevier Publishing Com., 1953.

38. F. Hoffmann and E. Mollow,
Z. Fuer. Angew. Phys., 14(2), 734, 1962.

39. F. A. Kröger and Mayer,
Physika, 20, 1149-56, 1954.

40. T. I. Barry and F. S. Stone,
Proc. Roy. Soc., 255(a), 124, 1960.

41. G. M. Schwab,
Adv. Catalysis, Vol. 9, Academic Press Inc., N.Y.

42. B. M. Arghiropoulos and S. J. Tischner,
J. Catalysis, 3, 477, 1964.

43. H.Z. Fritzsch,
Z. Physik, 133, 422, 1952.

44. W. D. Kingery and R. A. Mickelsen,
J. Appl. Phys., 37, 3741, 1966.

45. B. T. Kolomiets, T. N. Namontova and A. A. Babaev,
J. Noncrystalline Solids, 4, 289, 1972.

46. T. M. Donovan, W. E. Spicer and J. M. Bennett,
Phys. Rev. Letters, 22(20), 1058, 1969.

47. A. H. A Clark,
Phys. Rev., 154(2), 750, 1967.

48. A. I. Gubenov,
Quantum Electron Theory of Amorphous Semiconductors,
Trans. by A. Tybulewicz Consultants Bureau, New York 1965.

49. N. F. Mott and Davis, E. A.,
Phil. Mag., 22, 903, 1970.

50. G. Oster and M. Yamamoto,
J. Appl. Phys., 37, 823, 1966.

51. B. T. Kolomiets, T. N. Mamontova and G. I. Stepanov,
Sov. Phys. Solid State, 9, 19, 1967.

52. P. K. Chaudhari, E. R. Chenette and Van Der Ziel,
J. Appl. Phys., 43(7), 3150, 1972.

53. F. Stöckmann,
Z. Physik, 127, 563-78, 1960.

54. Prafulla Chandra, V. B. Tare and A. P. B. Sinha,
Indian J. Pure and Appl. Phys.,
5(8), 313-17, 1967.

(55) A.M. Peers,
J. Phys. Chem. 67(10),2228,1963.
(57) T. Kwan & Fujita Y.,
Bull. Chem. Soc. Japan 31, 379, 1958.
(58) V.A. Shuets, V.B. Kazansky.,
J. Catalysis. 25, 123-30, 1972.
(59) R.J. Kokes.,
J. Phys. Chem. 66(1), 99, 1962.

PART - II

CHAPTER - 1 - INTRODUCTION TO CdS

2.1.1. Cadmium sulphide is one of the most widely studied semiconductor mainly because of its photoconducting and semiconducting properties. It crystallizes in two forms[1]:

(1) Zinc blend structure
Cubic a = 5.82Å

(2) Wurtizite structure
Hexagonal a = 4.14Å, c = 6.72Å.

Crystalline thin films of cadmium sulphide are also found to have these two structures as revealed by the electron diffraction studies[2].

Cadmium sulphide is generally n-type as has been revealed by the work on thermoelectromotive force by many workers[3]. The band gap of cadmium sulphide has been reported mainly from the absorption studies. Though the values given in literature vary from 2.4 to 2.7 ev, 2.4 ev is the generally accepted value[4]. The absorption edge is found at 5100Å with a sharp cut off[5]. If the material is doped, then the edge may be shifted depending upon the dopants. The spectral response of sulphide has been studied and has the peak sensitivity in the visible range. Such study shows that the maximum photocurrent is observed approximately at the wavelength where maximum absorption takes place[6]. A typical room temperature value for electron mobility in CdS in dark is 200 cm^2/volt. sec.[4].

Cadmium sulphide has also been studied for its photoluminescence properties.

Photoconducting properties, luminescence and other properties have been explained with the help of the band diagram given in Figure 2.1. The location of impurity levels such as those arising from Ag, Cu, Cl, Br, I, Al, Ga and In have been experimentally determined[4]. Apart from the impurity levels present, some levels in the forbidden gap have been attributed to crystal defects. These levels affect the photoconducting properties to a large extent and therefore have been studied thoroughly. The presence of these levels has been shown from the study of glow curves and thermally stimulated current curves. Major levels found are at 0.05, 0.18, 0.23, 0.41, 0.63, 0.83 ev below the bottom edge of the conduction band[7].

CdS has found application as photoconductor because it has all the desirable properties of a good photoconductor which are:

(1) Sufficiently large band gap to provide the required high value of dark resistivity.

(2) The response in desired spectral range.

(3) A low density of trapping levels to permit the theoretical speed of response to be obtained at low light intensities.

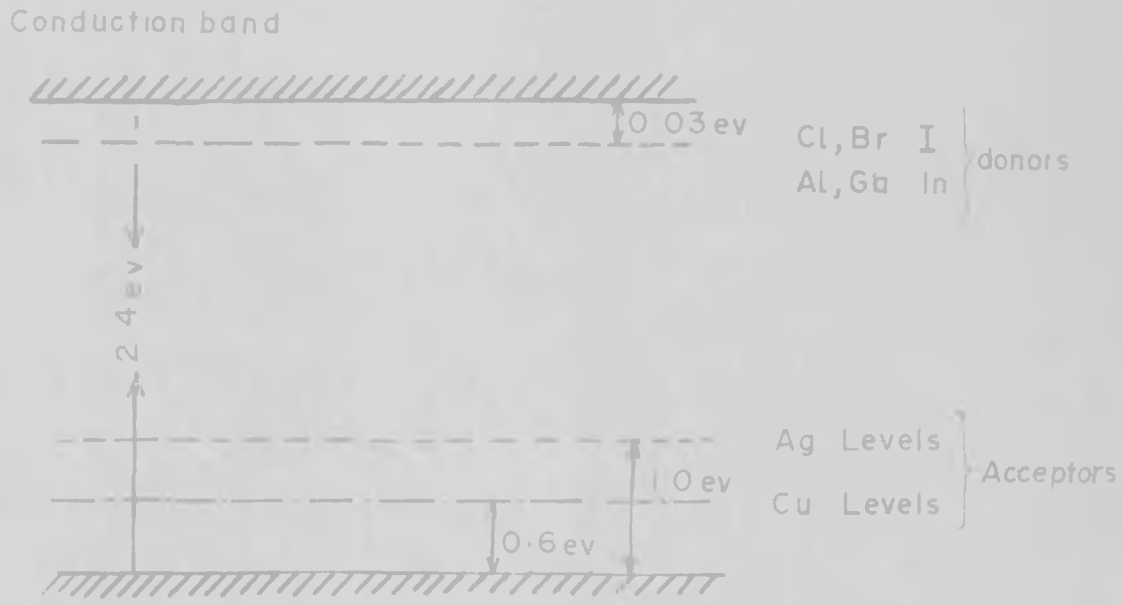

Fig 2 1 CdS BAND DIAGRAM WITH IMPURITY LEVELS

(4) A close control on the concentration and nature of defects to permit the exclusion of centers with a large recombination cross-section.

In view of all these desirable properties, thin films of CdS have been prepared by different methods; namely (1) vacuum evaporation, (2) vapour deposition, (3) sputtering, (4) chemical deposition and their properties studied thoroughly.

2.1.2. HISTORICAL REVIEW OF CdS THIN FILM STUDY

A lot of work has been done on evaporated films, powder sintered layers and single crystals of cadmium sulphide. The work upto 1955 has been reviewed by Bube[8]. Even today, a sufficiently large interest in the study of this material exists, because of its properties such as piezo-electricity[9], laser action[10], etc.

Evaporated thin films of cadmium sulphide are being studied since 1940s. Weiss[11] prepared the films by vacuum evaporation. Wlerick[12] studied the role of traps in the conduction mechanism in cadmium sulphide thin films. In addition, photoconductivity, as a function of illumination was studied by the same investigator.

The optical properties of thin films of cadmium sulphide were studied by Gottesman and Ferguson[13] in 1954. They studied

reflectivity of films at different wavelengths from 4000-7500Å. The refractive index was calculated. They reported that the more the rate of deposition of film, the more was the density of film material. Optical properties have also been reported by Hall et al.[14].

Aitchison[15] established the conditions to get photo-sensitive cadmium sulphide films. Forgue[16] reported that the dark resistance was lowered by heating the films which might be useful as detectors. "The impurities in cadmium sulphide to be evaporated affect the sensitivity and if it is pure then films obtained were sensitive" reported Bramley[17].

Bube et al.[18] studied the effect of impurities on spectral response of CdS. They reported that photocurrent varied as a square-root of light intensity. If 'Cu' impurities were more, current varied as the square of the light intensity.

Schwartz[19] described several variations in the evaporation procedure including sputtering and low voltage arc techniques of evaporation. Wlerick and Pregermain[20] showed that photocurrent-illumination graph was non-linear.

Gilles and Cakenberghe[21] studied evaporated layers of CdS. It was found that crystallization of layers gave better sensitivity. They also reported that less defects in the crystals and larger size of the crystals gave the highest photocurrent.

Lawrence[22] studied the films prepared by vacuum evaporation, sputtering the Cd film and heating in H_2S to get CdS film, and chemically deposited layers. The spectral response as a function of substrate temperature was reported. 'Cu' activated films evaporated on the substrate at 400°C gave faster response and better sensitivity. Films formed using sputtering technique showed no variation of time constant with illumination. Chemically deposited films had higher time constants. The square root increase in conductivity with illumination intensity, was reported.

Clayton et al.[23] studied the effect of x-ray and γ rays on the conductivity of CdS thin films. Their experiments supported the conception of photoconductive trapping and decay, as applied to the ionising radiation and falling on quasi-insulators. Veith[24] studied Cd-excess as well as Cu-doped CdS thin films. Log 1/T curves, spectral response and the effect of illumination intensity were studied. For undoped films the peak in the spectral response was reported at 500

Kozirev and Kusakin[25] showed that initial electrical conductivity in Cu activated CdS layers was increased by electron bumbardment. Shaw[26] studied and interpreted photoconductivity decay as a function of illumination intensity.

Zollei[27] prepared the films from CdS suspensions or CdS colloidal solution. Ammonium chloride or bromide or iodide were used as dopants. Photosensitive films were obtained by sintering. Effect of air oxidation was studied by Kitamura[28].

Shalimova and coworkers[29] studied the optical absorption in CdS thin films. "Careful experiments showed no evidence for possibility of forming cubic CdS films by any of the various methods of preparation", reported Ahlburg et al.[30].

Wendland[31] studied the structure, conductivity and optical transmission for vacuum evaporated CdS films. Dresner and Shallcross[32] worked on the several processing methods of CdS thin films and their effect on crystallinity, electronic properties, etc. Vecht[33] gave a new method of preparing crystalline CdS thin films in which he used organometallic compound in organic media as the starting material.

The dependence of electrical conductivity on different parameters such as temperature, ambient gas pressure, etc. was studied by Kiryashkena et al.[34]. A possible effect of the ratio of cubic to hexagonal phases on conductivity was discussed.

Shalimova and coworkers[35] studied the effect of substrate temperature on the structure of the deposited films. If the

substrate temperature was 120-250°C, then a mixture of cubic and hexagonal phases was obtained. From 200°C to 250°C, only hexagonal structure was observed. "Hexagonal structure had many packing defects" reported the authors.

Sakai and Okimura[36] studied evaporated films of CdS and found that they had the hexagonal structure and a good photosensitivity.

Lehmann[37] worked out the theory of optical absorption of CdS and ZnO. Voigt[38] studied the rise and decay curves from where he obtained and studied the nature of trapping in these films. Aramu et al.[39] reported the comparison of rise and decay curves in cubic and hexagonal CdS thin films. Anisotropy in the electrical properties in thin films of CdS was studied by Vergunas et al.[40]. They also reported the dependence of photosensitivity on substrate temperature and orientation.

Heyraud and Copella[41] showed that epitaxial films could be grown on cleavage faces of NaCl, KCl, by the vapour phase chemical reaction technique and also reported that the electrical and optical properties of these films were the same as those of the bulk material.

The effect of orientation on the properties of CdS has also been studied by Mingazin et.al.[42], Efremenkova et al.[43]. Lyabeheriko and Swechinkov[44] reported two types

of recombination centers in the vacuum evaporated films. The dependence of photoconductivity on intensity was studied by Bube[45], Vateva[46] and many others. The effect of trapping on photoconductivity was studied by Barbinchuk et al.[47] and Henry et al.[48]. Although CdS thin films are generally n-type, by using ion implantation technique, p-type CdS is reported to have been produced successfully. Hou[49] implanted p^+ in CdS and studied the photoelectronic properties. Other related topics such as infrared quenching, thermally stimulated current, space charge limited current, Hall effects, etc. have also been studied extensively by many workers. The study by Bube and coworkers has a unique importance in the field of photoconductivity in CdS.

We may summarise this background by the remarks that in general CdS films prepared by different methods generally show different properties. A slight variation of conditions in a method of preparation sometimes changes the properties considerably. It is, therefore, considered that a new method of preparation CdS thin films as is described in the next few pages would be interesting.

An important aspect of the present study is that the properties of thin CdS films having cubic structure are reported for the first time. CdS in the form of thin film reported so far

had hexagonal or the mixed (cubic + hexagonal) phase. Only Bube et al.[50] have reported photoelectronic properties on cubic CdS layers. Our method of preparation, however, has certain advantages. The film is uniform and requires no binder for the preparation.

CHAPTER - 2 - EXPERIMENTAL

2.2.1. PREPARATION OF THIN FILMS OF CADMIUM SULPHIDE

The preparation of thin films of cadmium sulphide was done by a method similar to that described earlier for ZnO.

A dilute solution of cadmium acetate (A.R. 1%) in distilled water was taken in a shallow dish. A glass plate was kept dipped in this solution with an arrangement to lift it out when desired. The assembly was enclosed in H_2S atmosphere for a few mimutes. It was observed that a continuous flow of H_2S did not give an uniform film. Instead a saturated solution of H_2S in water was enclosed within the assembly. A thin uniform layer of cadmium sulphide was then formed at the surface of the solution. Care was taken that no precipitation took place inside the solution.

The film formed by this procedure was transparent and very thin. To obtain thick films, the pH of cadmium acetate solution was adjusted and it was found that at pH 3.5, the films obtained were thicker, uniform and photosensitive. It showed relatively fast rise and decay.

The film thus formed was carefully lifted on a glass substrate kept inside the solution and then the glass slide was dipped in distilled water allowing the film of CdS to float on

the surface of water to remove the soluble impurities. This washing procedure was repeated two to three times. The film was finally collected on the desired glass substrate. It was dried and stored in dark in a dessicator.

2.2.2. For the measurements of electrical properties the ideal contact to semiconductors would be the one having the following properties:

(1) It should be highly conducting.

(2) Contact material should not react with the semiconductor material.

(3) Contact properties should not change with variations in temperature, illumination, electrical field and other ambient conditions.

The metal chosen should be such that its work function matches with that of semiconductor; then, if no oxide or any other layer is formed, between the metal and semiconductor, it would give an ohmic contact.

It is found that In, Ga, fulfil all the conditions to form an ohmic contact with CdS.

Following is the review of the work done on thin films of CdS related to its photoconducting properties.

2.2.3. ELECTRON DIFFRACTION STUDY

In order to know the structure of the film formed, the sample was examined by electron diffraction. The washed film floating on water, was picked up on a wire gauge. The wire gauge had a collodion film formed over it previously. The cadmium sulphide film after taking on wire mesh was dried and used for the electron diffraction study by transmission.

From the photographs the 'd' values were calculated. Calibration was done using the standard pattern of graphite.

2.2.4. DARK CONDUCTIVITY

For the measurements of dark conductivity the film was deposited on a glass slide (2.5 cm. x 1 cm.) as described earlier and the indium electrodes were vacuum deposited by the usual technique. The distance between the two electrodes was approximately 2 mm. The sample holder is shown in Fig. 2.2. It consists of two parts: Part A is made of brazing two concentric tube x and y. y is a long cylindrical tube closed at one end over which sample is fixed in close contact with its wall. Tube x has a flange in which a groove is made for an '0' ring and also holes for nut and screw arrangement. Another side tube z is fixed to x through which wires of the heater, thermocouple and those for measuring conductivity were brought out.

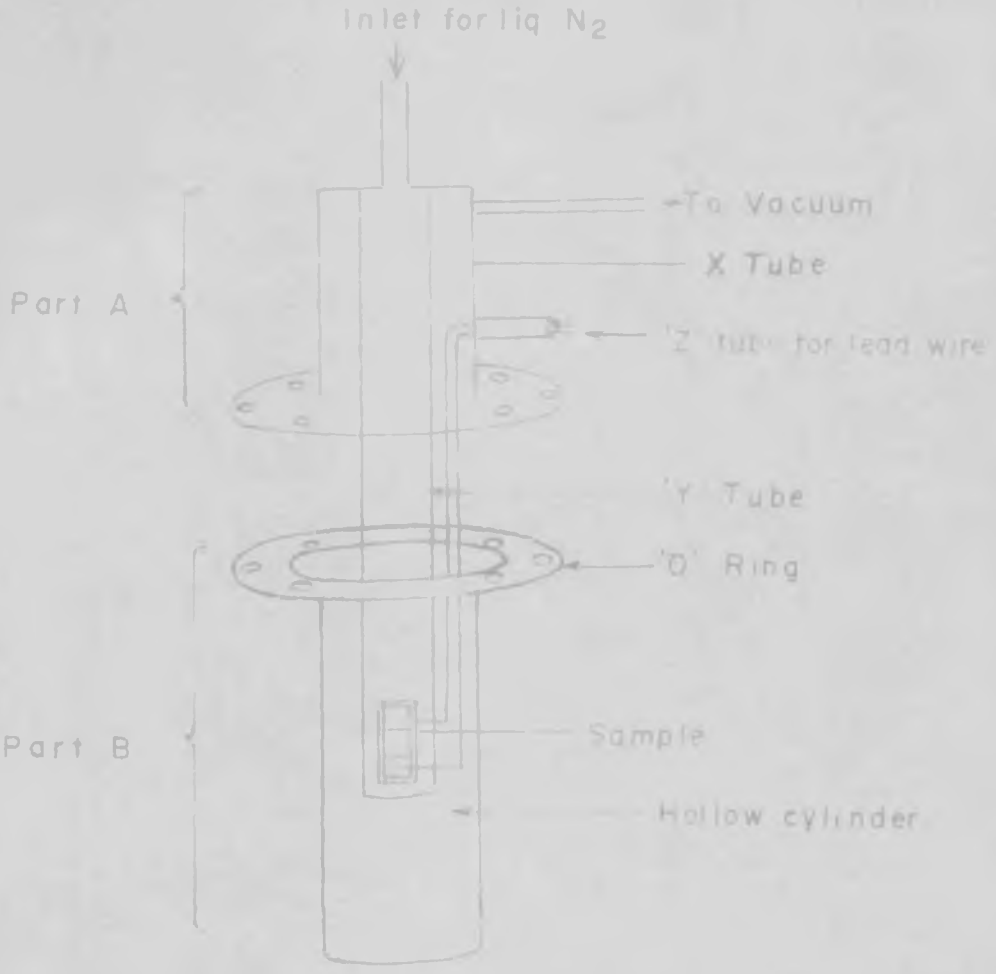

LOW TEMPERATURE DARK CONDUCTIVITY MEASUREMENT APPARATUS

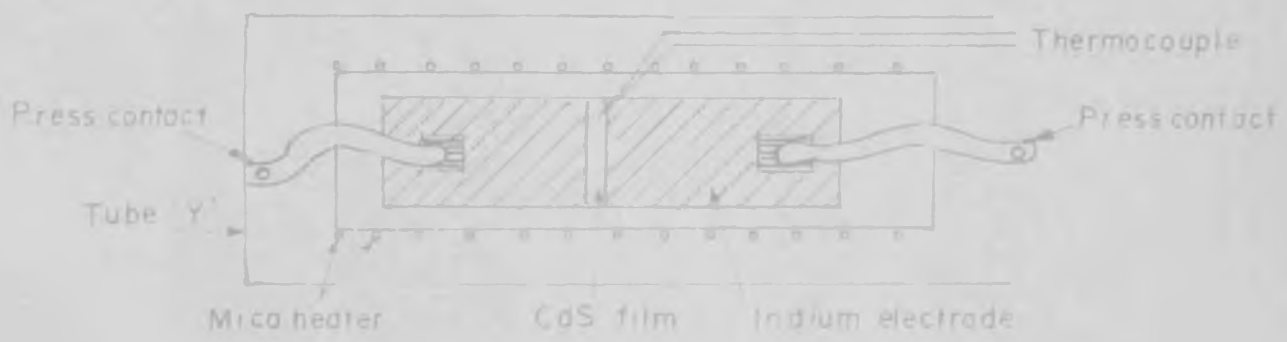

Fig 2 2

SAMPLE HOLDER FOR CdS THIN FILM

Part B consists of a hollow cylinder closed at one end and has a flange at the other end. When the parts A and B are fixed by screws it becomes a closed vacuum tight system.

A heater made by winding Kanthal tape on a mica sheet (kept insulated from the walls of tube y) was kept under the sample. Press contacts were used so that there was a minimum temperature gradient between the wall of the cylinder and the sample.

Measurements of resistance at different temperatures were done by using an RIE meter (Leeds and Northrup, Cat. 5620).

The sample was fixed in the sample holder and kept in vacuum overnight. Liquid nitrogen was poured through the inlet till the thermocouple showed a steady voltage. Sample holder acts as a metal thermos and liquid nitrogen remains in the tube for sufficient time to give a constant temperature. The resistance was recorded. As the liquid nitrogen evaporated, the temperature of the sample increased. The resistance was recorded at small intervals till room temperature was attained. Then the heater was switched on and the sample was heated. The resistance was thus recorded at temperatures higher than the room temperature.

The graph of log resistance vs 1/T was plotted which we used to calculate the activation energies in different temperature ranges.

2.2.5. LIGHT ABSORPTION

Films of CdS were deposited on the glass slides for optical measurements. The optical absorption was studied in the range 4000-7000Å, using a Unicam Spectrophotometer (Sp6000). The absorption was plotted as a function of wavelength. The thickness of the films was measured by recording the weight of the film. The absorption coefficient was calculated.

2.2.6. PHOTOCONDUCTIVITY RELAXATIONS

Slow photocurrent relaxation is of considerable interest as this phenomenon is sensitive to trapping effects.

The experimental arrangement for this measurement is shown in Fig. 2.3. The light source and the sample are kept at a fixed distance inside a closed box made up of metal sheets to avoid light on the sample. A slit in the box provides an arrangement to insert a filter in between the sample and the light source.

The sample was kept in dark for two hours before the actual measurements were done. The light source was put on and the change in the voltage across a resistance in series with the sample was recorded on a strip chart recorder with a response

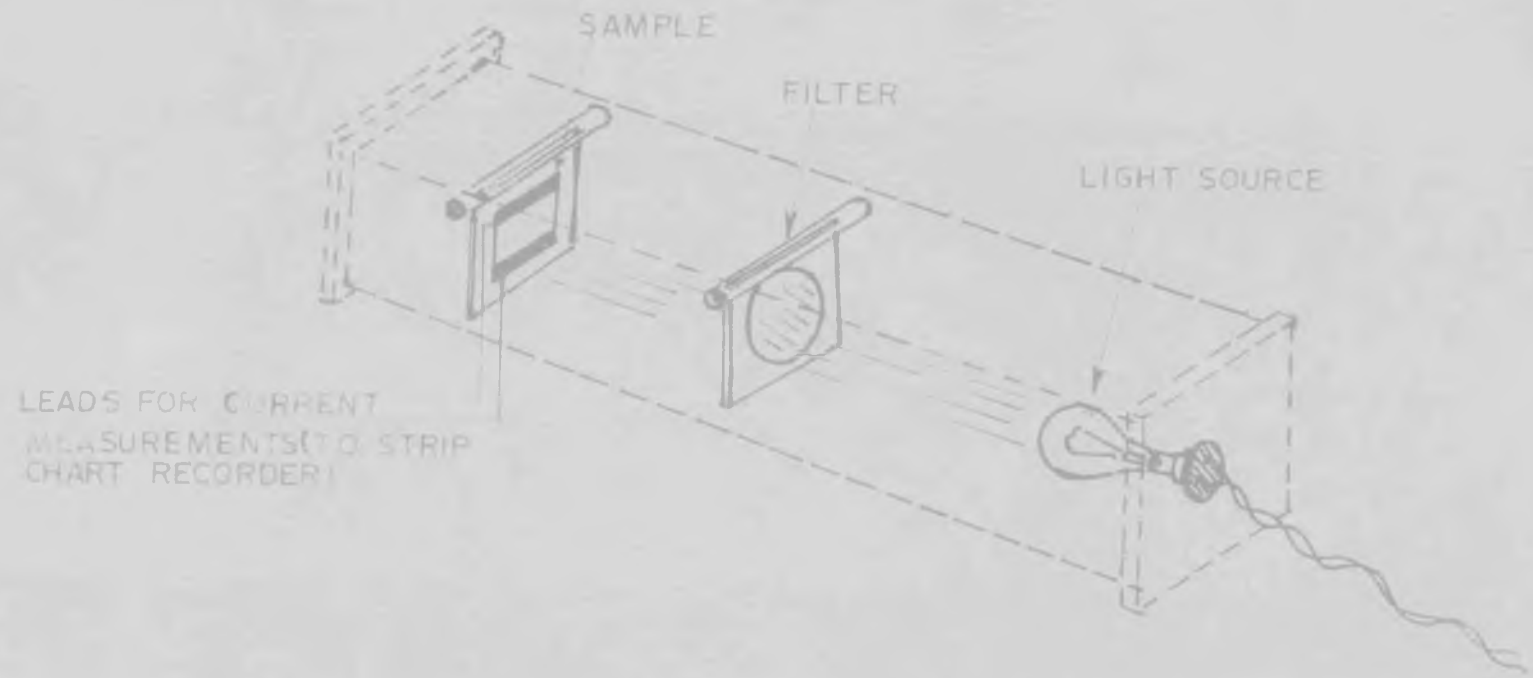

Fig 2.3 EXPERIMENTAL ARRANGEMENT FOR PHOTOCONDUCTIVITY RELAXATION CURVES OF CdS THIN FILMS

time of 0.5 sec. The sample was kept in light for a fixed duration (10 sec.) and then the light was put off. The drop in current was recorded for the same duration. A filter was then inserted which reduced the light intensity by 50%. Again the current was recorded for a fixed duration and then the light put off. The fall in current with time was also recorded. This procedure was repeated using the various neutral filters changing the intensity from 100% to 5%.

A graph of log current vs log intensity (arbitrary units) was plotted.

2.2.7. SPECTRAL RESPONSE

The spectral response measurements of the CdS films were done at room temperature using the Unicam Spectrophotometer. A special sample holder was made for this purpose, so that the sample could be kept at the desired place. Leads to measure the resistance of the CdS film were taken out taking care that no stray light fell on the sample.

The resistance was recorded at different irradiation wavelengths from 4000Å to 7000Å.

A graph of resistance as a function of wavelength was plotted.

CHAPTER - 3 - RESULTS

Figure 2.4 shows the electron diffraction (transmission) pattern for the CdS film along with the graphite pattern for calibration.

The following table gives the 'd' values and relative intensities for various lines for ∝(hexagonal) and β(cubic) forms of cadmium sulphide from the literature and also the observed 'd' values and intensities for our sample.

CdS ∝		CdS β		Experimental	
'd'	I/I_o	'd'	I/I_o	'd'	Intensity
3.65	80	3.36	100	3.33	Very strong
3.32	60	2.06	100	2.04	Very strong
3.12	100	1.76	90	1.75	Strong
2.42	60	1.34	30	1.34	Weak
2.06	90	1.12	40	1.11	Weak
1.89	90				
1.75	80				
1.32	60				
1.16	60				

Our pattern matches with that of β CdS(cubic).

The calculated value of a = 5.87A.

Fig. 2.4. Electron diffraction pattern (transmission) of CdS thin film.

DARK CONDUCTIVITY MEASUREMENTS

The plot of log R vs 1/T as shown in Fig. 2.5 shows the behaviour of CdS thin films. The important observations are: (1) at low temperatures from -130°C to +6°C, the resistance decreases very slowly. The activation energy calculations show that ΔE = 0.022 ev, and (2) from +6°C to 100°C, there is a steep decrease in the resistance with the activation energy = 0.90 ev. The impurity conductivity characteristics are shown in the whole region of measurements i.e. from -130°C to + 100°C. The change in conductivity at +6°C is sharp indicating a descrete impurity level in the forbidden gap.

ABSORPTION IN THE VISIBLE REGION

The absorption wavelength curve (Fig. No. 2.6) shows a sharp change at 470 mμ and also from the calculations of absorption coefficient we can see that the coefficient is of the order of 3.5×10^4 at 460 mμ (measurements at 300°K).

SPECTRAL RESPONSE

The plot of resistance as a function of wavelength is shown in Fig. 2.7. A clear minimum is shown at the wavelength 430 nm at 300°K (Fig. 2.7).

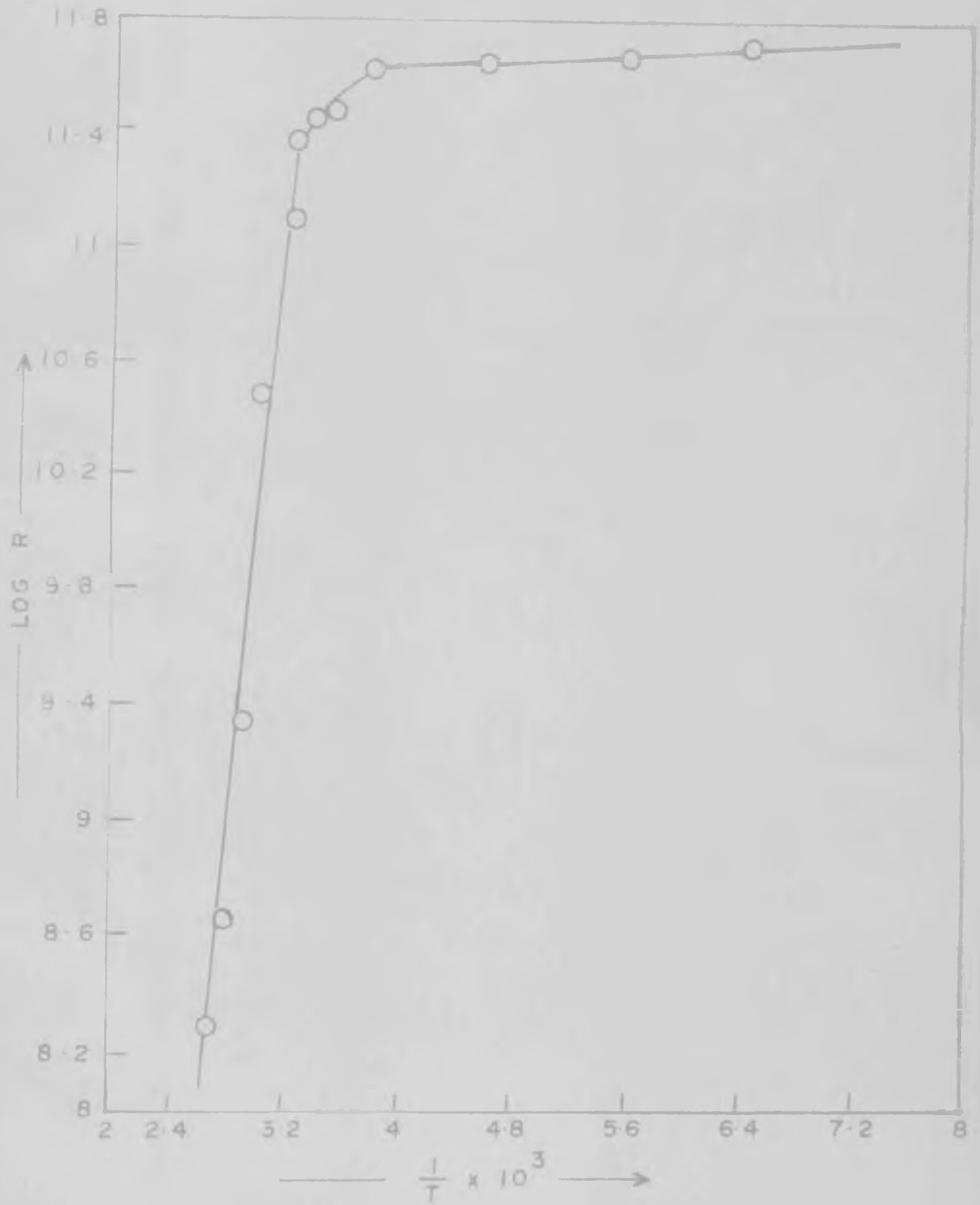

Fig 2·5 LOG DARK RESISTANCE Vs $\frac{1}{T}$ PLOT FOR CdS THIN FILM

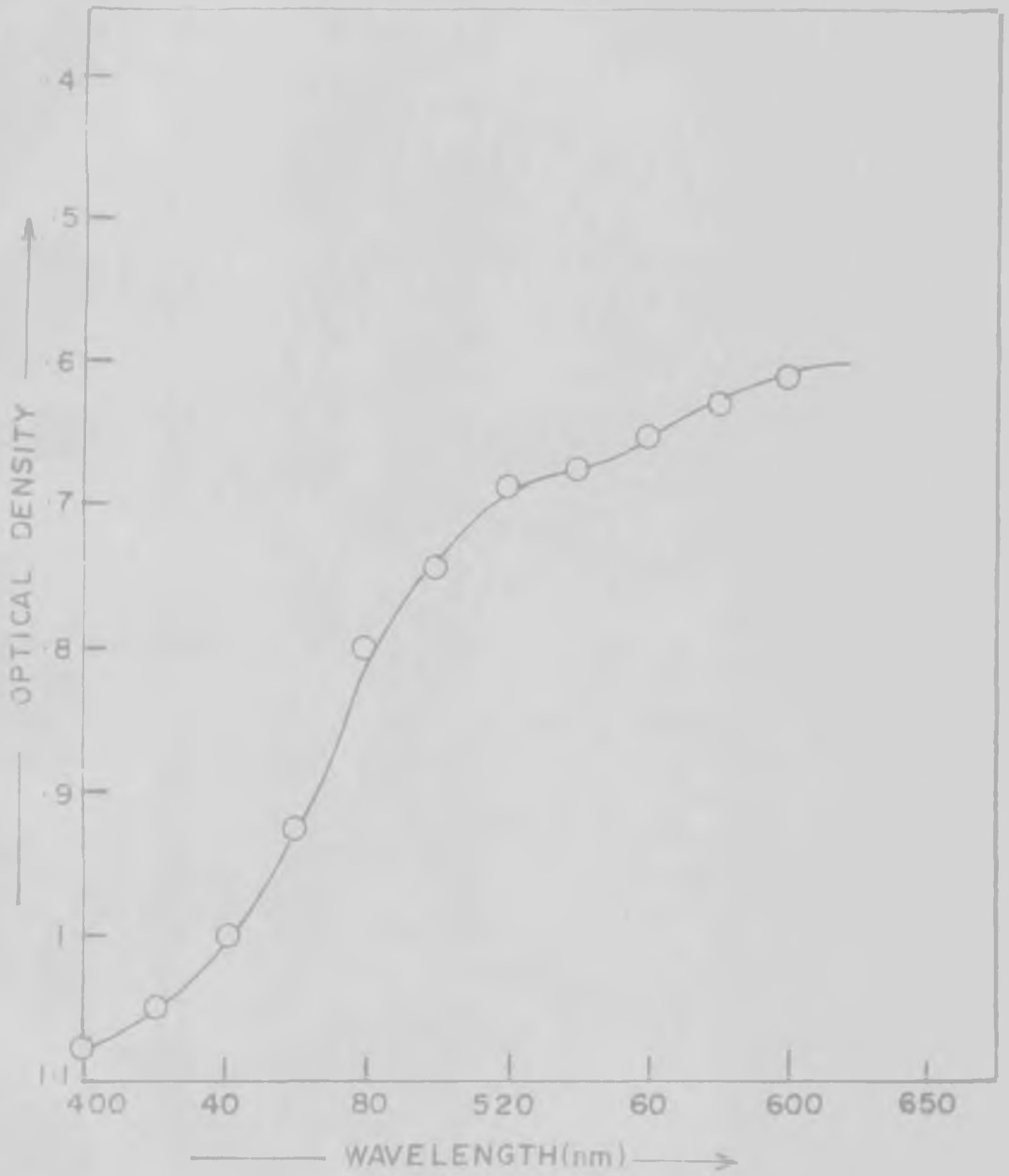

Fig 2·6 . ABSORPTION OF CdS FILM

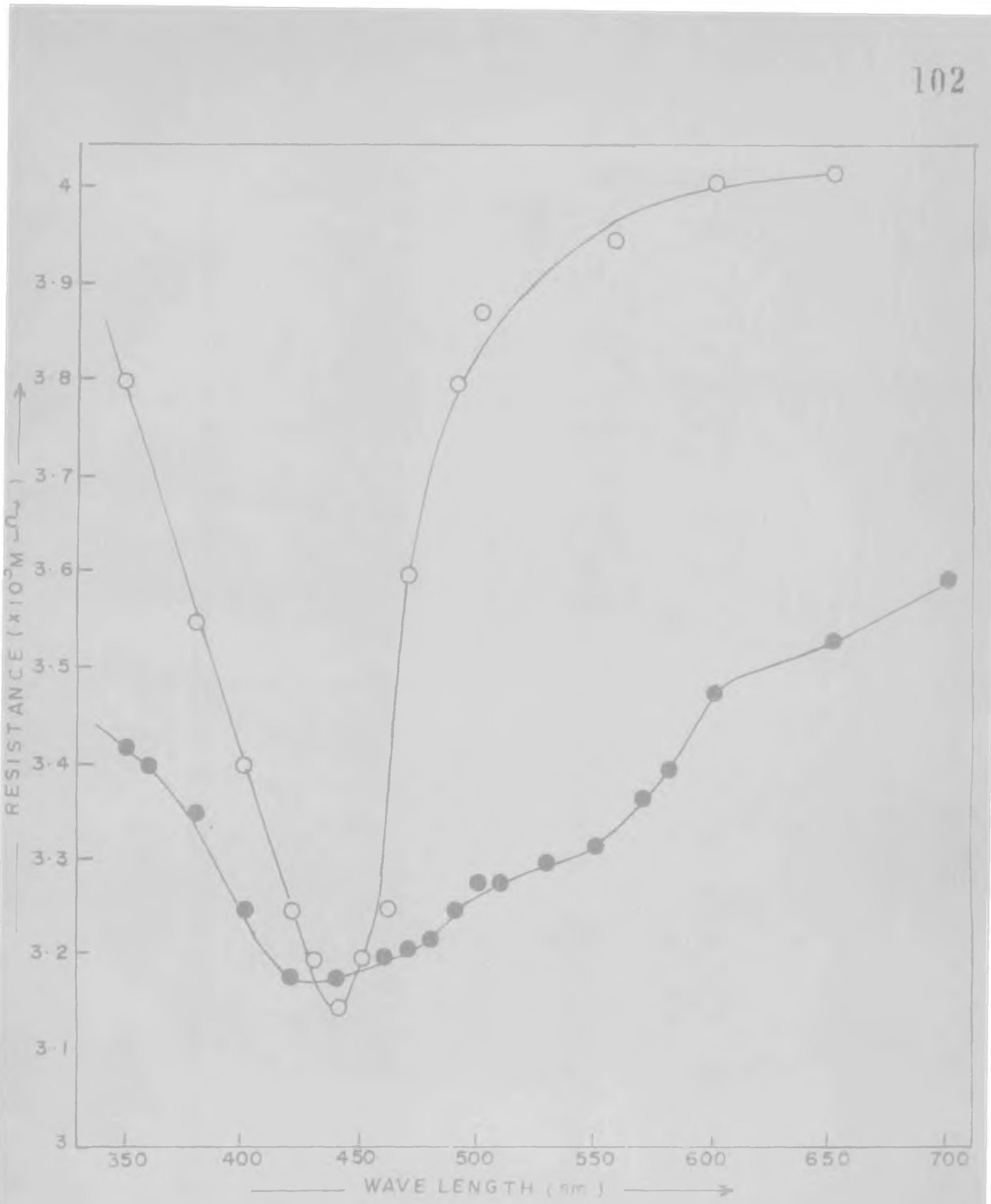

Fig 2-7 SPECTRAL RESPONSE FOR CdS THIN FILMS

RELAXATION

Slow photoconductive relaxation curves are shown in Fig. 2.8. The recording is done at 300°K at various light intensities. As is clear from the curve, the initial rise is very fast and reaches the saturation value in a period very small compared to the irradiation time. The order is of microseconds. When the light is put off, the current initially falls sharply and then a rather slow change is observed.

It can be noted that no two distinct slopes can be observed in the rise and decay curves.

The current variation with light intensity is shown in the graph of log current vs log light intensity in Fig. No. 2.9. The slopes of the lines are 0.43 and 1.33.

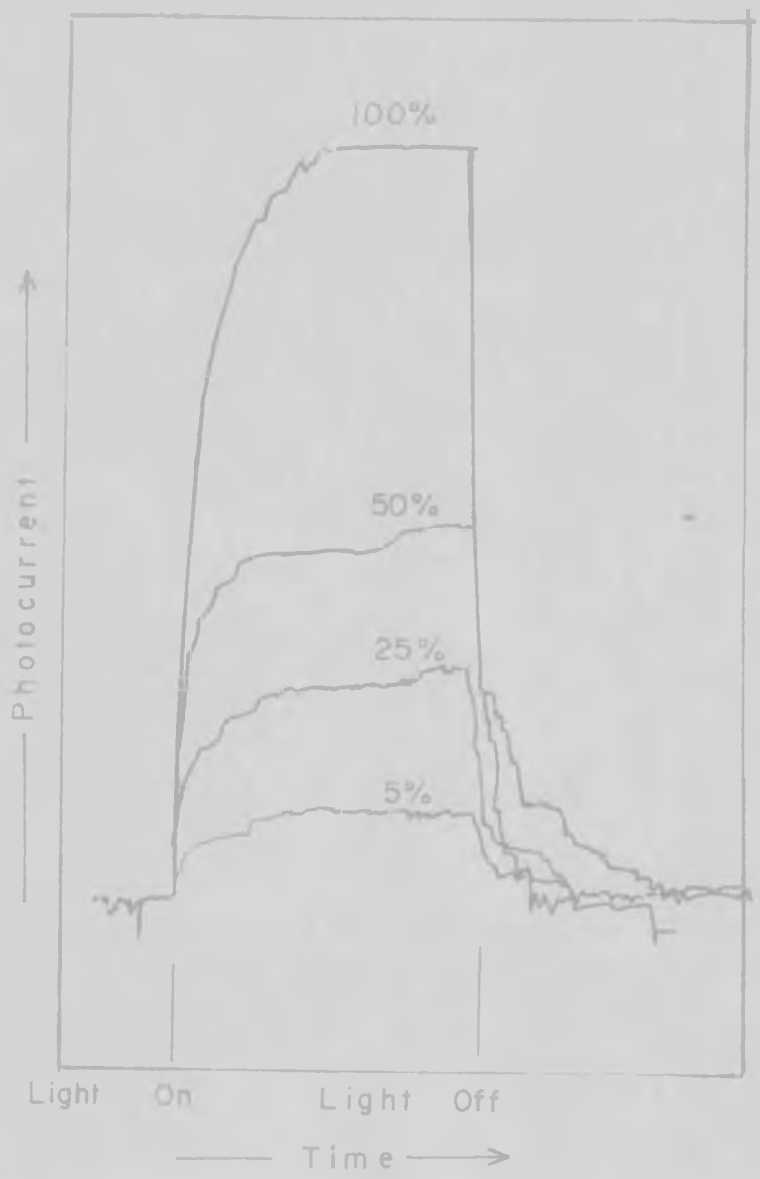

Fig 2·8 PHOTO CONDUCTING RELAXATION CURVES AT ROOM TEMP
AT DIFFERENT LIGHT INTENSITIES

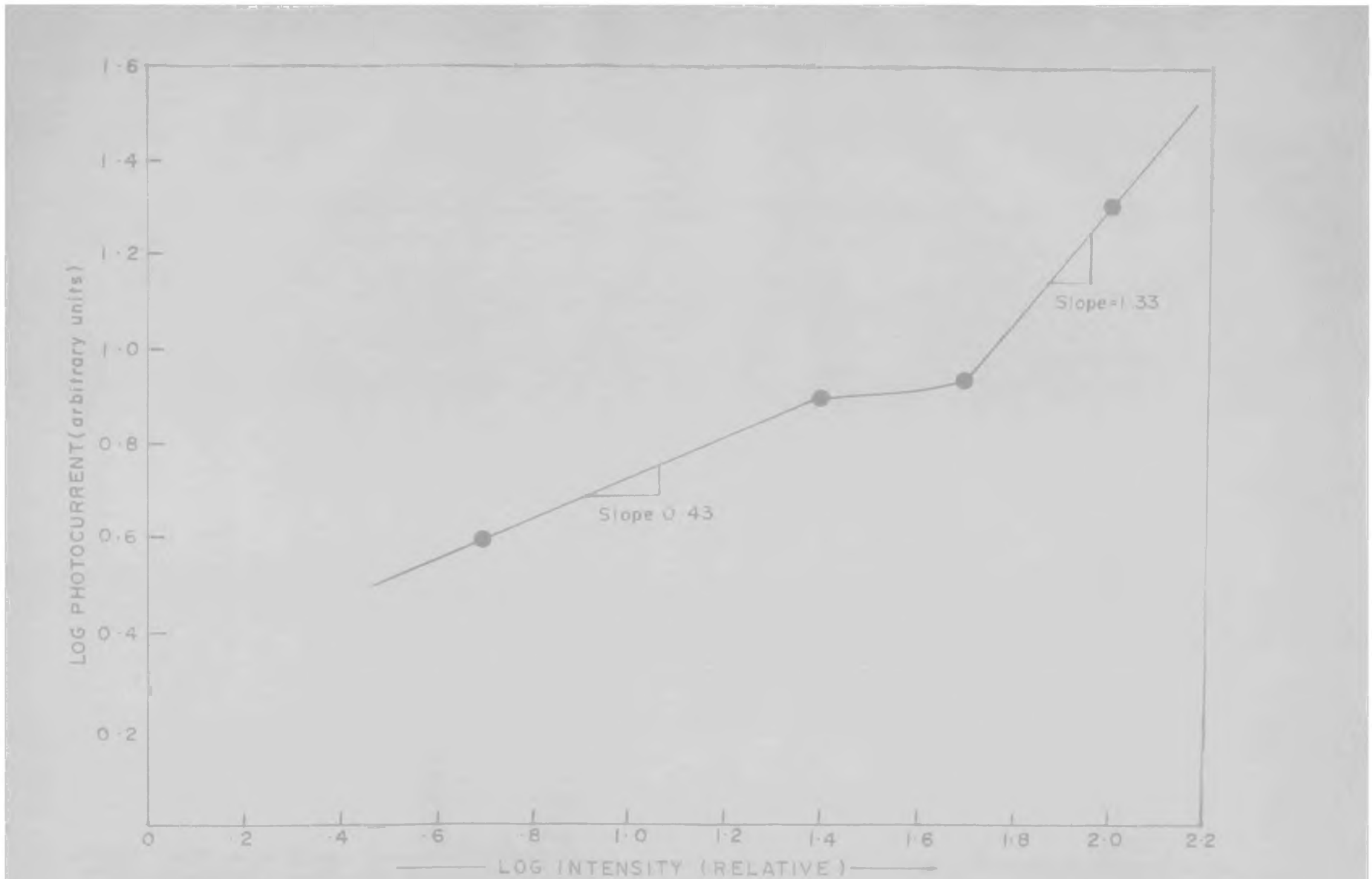

Fig. 2·9 PHOTOCURRENT Vs. ILLUMINATION CHARACTARISTICS OF CdS FILMS

CHAPTER - 4 - DISCUSSION

The important points to be discussed are:

(1) The feasibility of the method described as the general method of preparation of sulphide thin films.

(2) The properties of CdS thin films prepared by this method dye.

(a) Cubic structure from electron diffraction studies.

(b) Dark conductivity curve showing two trap levels at 0.022 ev and 0.9 ev.

(c) Photoabsorption in the visible region showing the absorption edge at 470 nm.

(d) Spectral response curve, i.e. R vs light wavelength, showing minimum at 430 nm.

(e) Photoconducting relaxation curves at different light intensities at room temperature showing the presence of shallow traps.

(f) Variation of photoconductivity as a function of light intensity showing sublinearity at low light intensities and superlinearity at high light intensities.

It is observed that the pH of the starting solution determines the properties of CdS thin films. Primarily, the pH is found to affect the composition and the crystallinity of the deposited film. The variations in these properties, in turn, affect the semiconducting and photoconducting properties. When

the pH is near 7, the film obtained is very thin and transparent. Such films also show photoconductivity without any intentional doping. Probably, excess 'Cd' is present in these films.

As the initial solution is made acidic, i.e. when the pH is decreased, the films formed are yellow, thick and uniform with moderate transparency. These films may have less excess Cd. Also the crystallinity may increase with acidity of initial solution.

Highly acidic solutions give CdS films which are reddish in colour. The red colour has been attributed to polymerised CdS aggregates, as reported by the earlier workers[51]. Our measurements on such films show that these films have slow response for rise and decay in photoconductivity curves. More defects are probably present in these films causing more levels in the forbidden gap.

All these films obtained showed 'n' type conductivity. If we compare these results with the ones reported by Wendland[31], it appears that the decrease in pH in the present method has the same effect as the increase in the substrate temperature or the decrease in the source temperature has for the evaporated film. The temperature of the initial solution, however, did not show any effect on the properties of the films obtained.

Vapour deposited CdS films have been extensively investigated by x-ray or electron diffraction techniques. When crystalline, the reported phase, is mostly having hexagonal structure. Escoffery[52], under controlled conditions of vapour deposition has reported cubic phase in CdS films. Mixed phase containing cubic and hexagonal phases in chemically deposited films is reported by Menezes et al. Vapour deposited mixed phase is also reported. CdS precipitated from $CdSO_4$, $Cd(NO_3)_2$ has a cubic structure while that from $CdCl_2$ gives the hexagonal phase[53].

Escoffery[52] evaporated indium doped CdS single crystals at 750°C for 30 minutes on to 51 μ thick (200) oriented molybdenum foil held at 175°C. A thick transparent deposited layer 120 μ thick showed single line in the x-ray reflection photograph. Also, he reported that CdS evaporated at 870°C on a substrate, freshly cleaved muscovite mica, (76 μ) was highly oriented and showed two lines in the x-ray reflection photograph corresponding to hexagonal (002) and (004) reflections. He observed that the (002) reflection was always accompanied by (004) even after conditions of film formation were slightly varied.

The major difficulty in determining the structure has been due to the inability to record enough number of lines. For the few major lines the 'd' values for the structure are so close that it is often difficult to ascertain the nature of the phase.

In our sample it can be easily seen that all the calculated 'd' values match with the 'd' values reported in the ASTM cards for the cubic CdS. Furthermore, if the sample had been in hexagonal phase the order in which the lines intensities are expected is not present. On the other hand, the visual observation confirms that the line intensities also match to those expected for the cubic cadmium sulphide phase. The log dark resistance vs 1/T plot shows two straight lines having different slopes indicating that two discrete levels are present in the forbidden gap.

The calculated activation energy values are 0.022 ev and 0.9 ev which are comparable to the reported shallow traps at 0.05 ev and 0.83 ev, by Woods et al.[7] from the conductivity glow curves.

Cd rich samples are reported to show these two traps. Also, such levels are likely to be due to donor impurity present in CdS crystals. These traps may be due to sulphur vacancy.

The spectral absorption edge for the layers as determined on a spectrophotometer is at 480 nm at room temperature. For the undoped hexagonal single crystals, the spectral absorption edge is reported at 500 nm to 520 nm.

In our samples the edge is obtained at 470 nm. Moreover, it may be noted that the structure of cadmium sulphide films in our experiments is cubic. Data for the cubic cadmium sulphide thin films is not available in the literature except that from Bube et al.[50] who have reported the spectral response results on CdS(cubic)layers.

Bube et al.[50]prepared their sample by mixing the powder with the binder of ethyl cellulose in amyl acetate and the layers fired at 240°C and 450°C respectively. The CdS powder was previously prepared by precipitating $Cd(SCH_3)_2$ by bubbling CH_3SH through the .1 M solution of cadmium acetate and then decomposing the product at 198°C. Sample fired at 240°C was cubic showing the edge in the spectral response study at 2.1 ev while the one fired at 450°C was mainly hexagonal showing the edge at 2.4 ev.

Menezes et al.[54] reported the spectral response peak for the chemically deposited CdS layers at 480 nm, matching with the absorption edge in their samples. It was also reported that the cadmium sulphide in their samples had a mixed phase having cubic and hexagoanal forms.

Fig.2.7 shows that in our sample the maximum response is obtained at about 430 nm. This is not in agreement with Bube et al.[50] and Meneses et al.[54]. The change in the photo-

electronic band-gap may be due to the small particle size as was suggested by Bube et al.[50], but it may be noted that in all the experiments mentioned above cadmium sulphide was prepared by chemical precipitation methods and therefore such a large difference in particle size is not expected so as to cause the change of > 50 nm in spectral response peak values. Menezes et al.[54] suggest this shift as due to bound excitor structure or to increased life time of photoexcited carriers at the surfaces.

We attribute this to the cubic structure of the films. Our results of photoabsorption show that the edge is at 470 nm corresponding to the band gap 2.6 ev. This value is very much higher than the single crystal (hexagonal) value of 2.4 ev at room temperature. Further shift to lower wavelength may be due to the band exciton transition and hence the photoconductive response peak at 430 nm. If the cubic phase in the samples of Menezes et al. contributes in the spectral response, their observations are consistent with the proposed idea.

The rise and decay in photoconductivity relaxation curves show that, for all the intensities, the rise time and decay time are short of the order of mili seconds.

Initially there is a fast rise in photocurrent and then the rise is more gradual. The equilibrium value is finally attained in a few seconds. In the decay curve also, initially, the

current is lowered sharply immediately after the light is put off and after some time, slowly to the dark current value of the film. This shows the presence of shallow traps. When the light is made on, electrons are pumped in the conduction band. Also, the shallow traps are filled. After an equilibrium is attained the saturation current is shown by a straight line. When the light is put off, electrons promoted from the valence band to the conduction band are stopped lowering the current. This lowering is not upto the dark current value as the shallow levels at room temperature make electrons available for conduction. This current decays gradually as the traps get emptied.

Figure 2.19 shows that at low intensities, sublinear photoconductivity (slope = 0.43) is observed while at higher intensities superlinearity is observed (slope 1.33). Avinor[55] has reported superlinearity in CdS single crystals (slope 1.34) comparable to our results.

This is explained on the basis of traps present in the forbidden gap. As the electrons are generated (by irradiation) in the conduction band, some of them are trapped. Since at room temperature, the shallow traps level is in equilibrium with the conduction levels, trapped electrons may be promoted in the conduction band as the free carriers. This means that the only

effect of traps present in forbidden gap very near the bottom of conduction band is to reduce the life time of the carrier. Thus a fraction power variation of current with light intensity is obtained at low intensities.

However, at higher intensities the number of free electrons generated is very high. Traps will be completely filled and it will have no effect on the carrier life time as described above. Also, Woods et al.[7] reported the photochemical changes in CdS and the part taken by the levels at 0.83 ev. This may be equivalent to the two classes of levels having different electron capture cross sections. After irradiation, as suggested by Rose[56], levels having high capture cross section may be modified into levels having low cross section, increasing the free electron life time. This may be the cause of superlinearity at higher intensities.

REFERENCES

1. Wyckoff, R. W. G.,
Crystal Structure, Vol. 1,
Interscience Publishers Inc. New York, 1951.

2. P. S. Aggarwal and A. Goswami,
Ind. J. Pure and Applied Phys., 1, 366, 1963.

3. F. A . Kröger, H. J. Vink and J. Volger,
Physica, 20, 1095-9, 1954.

4. R. H. Bube,
Photoconductivity of Solids,
230 (33), John Wiley and Sons Inc., 1960.

5. M. Balkanski and I. Broser,
Z. Elektrochem., 61, 715 (1957).

6. W. Veith,
Z. Angew Physik, 7, 1, 1955.

7. J. Woods and K. H. Nicholas,
Brit. J. Appl. Phys., 15, 1361, 1964.

Ibid., 15, 783, 1964.

8. R. H. Bube,
Proc. IRE, 43, 1848, 1955.

9. A. Doi and T. Ogawa,
Jap. J. Appl. Phys., 9, 723, 1970.

10. C. E. Hurwitz,
II-VI Semiconducting Compounds,
1967 International Conference,
p. 682, edited by D. G. Thomas,
Bell Tel. Lab., W.A.Benjamin, Inc., New York.

11. K. Weiss,
Z. Naturforsch., 2A, 650, 1947.

12. G. Wlerick,
Compt. Rend., 239, 257, 1954.

13. J. Gottesman and W. F. C. Ferguson,
J. Optical Soc. Amer., 44, 368, 1951.

14. J. F. Hall and U. F. C. Ferguson,
J. Optical Soc. Amer., 45, 714, 1955.

15. R. E. Aitchison,
Nature, 167, 812, 1951.

16. S. V. Forgue, R. R. Goodrich and A. D. Cope,
R. C. A. Rev., 12, 335, 1957.

17. A. Bramley,
Phys. Rev., 25, 246, 1955.

18. H. H. Bube and S. M. Thomsen,
Rev. Sci. Instr., 26, 664, 1955.

19. B. Schwartz,
Nature, 162, 614, 1948.

20. G. Wlerick and Pregermain,
J. Phys. Rad., 15, 757, 1954.

21. J. M. Gilles and J. Van Cakenberghe,
Nature, 182, 862, 1958.

22. R. Lawrance,
Brit. J. Appl. Phys., 10, 298, 1959.

23. C. G. Clayton, B. C. Maywood, J. F. Fowler,
Nature, 183, 1112, 1959.

24. W. Veith,
Compt. Rend., 230, 947, 1950.

25. B. P. Kozyrev and V. F. Kusakin,
Izvest. Vysshikh Uchels Zavedenii Fiz.,
2, 16, 1959; C.A. 8303 c, 1960.

26. D. Shaw,
Brit. J. Appl. Phys., 12(7), 337, 1961.

27. M. Zollei,
Acta Phys. Chem. Szedeg., 3(1-4), 21, 1957.

28. S. Kitamure,
J. Phys. Soc. Japan, 15, 1697, 1960.

29. K. V. Shalimova, T. S. Travina and Golik, L. L.,
Sov. Phys. Dockady, 6(5), 396, 1961.

30. H. Ahlburg, R. Caines,
J. Phys. Chem.(USA), 66(1), 185-6, 1962.

31. P. H. Wendland,
J. Opt. Soc. Amer., 52, 581, 1962.

32. J. Dresner and F. V. Shallcross,
J. Appl. Phys. 34(8), 2390, 1963.

33. A . Vecht,
Phys. Status Solidi, 3(7), 1238, 1963.

34. Z. I. Kiryashkina, V. A. Nozova and N.M.Luchanskaya,
Semicond. Materials Conf. Moscow, p. 77.

35. K. V. Shalimova, T. S. Travina and R.R. Rezvyi,
Sov. Phys. Dockady, 6(5), 404, 1961.

36. J. Sakai and H. Okimura,
Jap. J. Appl. Phys., 3, 144, 1964.

37. W. Lehmann,
J. Electrochem. Soc., 112(11), 1150-51, 1965.

38. J. Voigt,
Phys. Status Solidi, 12(1), 191-202, 1965.

39. E. Aramu, P. Manca, C. Muntoni,
Phys. Lett.(Netherlands), 19(8), 638, 1966.

40. F. I. Vergunas, T. A. Mingazin, E. M. Smirnova
and S. Abdiev,
Sov. Phys. Cryst.(USA), 11(3), 420, 1966.

41. J. C. Heyraud and L. Copella,
J. Cryst. Growth (Netherland), 2(6), 405, 1968.

42. T.A. Mingazin, E. M. Smirnova,
Kristallographia USSR, 14(2), 366, 1969.

43. V. M. Efremenkova, I. V. Egorova, V. E. Yurasova,
Izve. Akad. Neuk SSR Ser.Fiz., 32(7), 1242, 1968.

44. S. V. Svechinkov and A. V. Lyubchenko and E. B. Kaganovich,
Fiz. Tekn. Poplupravodnikov USSR 2(9), 1392, 1968,
Physics Abstracts, 10068, 1969.

45. R. H. Bube,
J. Appl. Phys. 41(6), 2751, 1970.

46. E. L. Vateva,
C.R. Acad. Bulg. Sc.(Bulgeria), 24(1), 11, 1971.

47. Babinchuk, V.V. Serdyuk,
Phys. Status Solidi A., 6(2), pk.81-4, 1971.

48. C. H. Henry, J. W. Shiever and K. Nassau,
Phys. Rev. B, 4(8), 2453, 1971.

49. M. Hou,
Appl. Phys. Lett., 16(11), 467, 1970.

50. R. H. Bube and E. L. Lind.,
J. Chem. Phys., 37, 2499, 1962.

51. J. W. Mellör,
Treatise on Inorganic Chemistry,
Vol. 4, p. 593, Longmans Green and Co. Ltd., 1930.

52. C. A. Escoffery,
J. Appl. Phys. USA, 35(7), 2273, 1964.

53. R. Sato, S. Yamashita and H. Ito,
Jap. J. Appl. Phys., 3(10), 626, 1964.

54. C. A. Menezes and N. Pavaskar,
Jap. J. Appl. Phys., 9(2), 212, 1970.

55. M. Avinor,
Phillips Res. Rep., 14, 211, 1959.

56. A. Rose,
Phys. Rev., 97, 322, 1955.

---000---

SUMMARY

ZINC OXIDE

Zinc sulphate solution, when enclosed in ammonia atmosphere, forms a film of zinc hydroxide at the surface of the solution. Such films were taken on silica substrates and heated at 140°C, 340°C, 450°C, 850°C and 1000°C to form zinc oxide films. The sample heated at 140°C, 340°C did not show any sharp x-ray diffraction pattern. Very faint lines were observed in x-ray pattern of the material formed by heating at 450°C. The material formed at 850°C and 1000°C, however, showed the typical ZnO pattern. From these observations, it was concluded that upto 450°C the films were amorphous.

Thermogravimetric study of the film material showed that there were major losses in weight at 125°C and 850°C while some minor losses in weight occurred in between these temperatures. This was explained by the following reactions:

First major loss

$$Zn(OH)_2 \longrightarrow ZnO + H_2O.$$

Second major loss at 850°C

$$ZnO.CO_{2(\text{ads. or otherwise})} \longrightarrow ZnO + CO_2.$$

The ultraviolet absorption by these zinc oxide films had been studied. The film heated at 850°C showed the absorption

edge matching to the stoichiometric zinc oxide single crystal absorption edge (385 mm). The films heated at 340°C and 450°C showed the absorption edge at a lower wavelength (365 ± 5 mm).

The electrical conductivity measurements on these films were done in air and also in hydrogen and oxygen. The following points are noteworthy:

CRYSTALLINE FILMS FORMED AT 850°C AND 1000°C.

(1) A maximum and a minimum are present in the log R vs 1/T curve for a fresh sample.

(2) Sample, once heated to 500°C in air, does not show such a maximum and minimum. However, just by wetting this film with water, its conductivity characteristics are recovered.

(3) Conductivity of the film is very much dependent on the ambient gas present. The conductivity is decreased in oxygen atmosphere; on the other hand, hydrogen increased the conductivity.

(4) In the temperature range of 25°C to 150°C, the impurity level located a depth of 0.03 to 0.05 ev from the bottom of conduction band dominates, while in the range 150°C to 500°C, the level at 0.8 ev controls the conductivity.

AMORPHOUS FILMS

(1) No maximum or minimum is present in the log R vs 1/T curve.

(2) Ambient gases are not found to affect the conductivity of these films.

(3) The log R vs 1/T curve shows that 0.8 ev level controls the conductivity right from room temperature onwards.

A suitable mechanism for conduction which could explain all these results has been suggested.

CADMIUM SULPHIDE

Cadmium acetate solution was enclosed in the H_2S atmosphere and the film formed at the surface of the solution was collected on the glass substrates for the study.

Transmission electron diffraction pattern was obtained for the film and 'd' values were calculated using the graphite pattern for calibration. The 'd' values matched well with the β CdS(cubic).

The films formed when the initial pH of the solution was 3.4 were uniform, transparent and had a fast photo response.

The dark conductivity was studied in the temperature range -100°C to + 100°C. The log R vs 1/T curve showed two straight lines having slopes 0.03 - 0.05 ev and 0.9 ev. This showed that two discrete levels are present in the forbidden gap of CdS band structure. These are comparable to the values of 0.05 ev, 0.83 ev, reported in the literature.

All the films obtained were photosensitive. Spectral response study showed that the maximum in response obtained was at 430 nm. This result is not in agreement with the one reported by Bube for cubic CdS layers where maximum sensitivity is shown at 590 nm.

The optical absorption in the visible range has also been studied. Optical density vs wavelength curve shows the optical absorption edge at 470 nm. The possible explanation for such high energy value is presented. Photoconductivity relaxation study was carried out to know the nature of traps present in CdS. The curves showed, initially, a fast response for rise and decay when the light is just put on and off respectively; and then a gradual change is observed. The analysis of the curves showed that the shallow traps are present in the forbidden gap at a depth of 0.022 ev levels as shown in the dark conductivity curve. The sublinearity at low light intensities and superlinearity at high light

intensities shown in log photocurrent vs log intensity curve have been studied and the possible cause for these has been suggested.

The study in this thesis shows that, this new method of preparation of thin films is useful to get stoichiometric amorphous thin films of ZnO and may be of importance in the study of amorphous to crystalline transitions in other oxides as well. It has been shown that the cadmium sulphide has properties different from those shown by the films prepared by the conventional methods. This may be true in other sulphides also. Thus, we feel that there is enough scope for carrying out further research in this direction.

---000---